TU/e EINDHOVEN UNIVERSITY OF TECHNOLOGY

In-duct and radiation matching strategies : preliminary report : TurboNoiseCFD Workpackage 2, Deliverable D2.3

Citation for published version (APA):
Rienstra, S. W., & Zhang, X. (2001). *In-duct and radiation matching strategies : preliminary report : TurboNoiseCFD Workpackage 2, Deliverable D2.3*. (RANA : reports on applied and numerical analysis; Vol. 0110). Technische Universiteit Eindhoven.

Document status and date:
Published: 01/01/2001

Document Version:
Publisher's PDF, also known as Version of Record (includes final page, issue and volume numbers)

Please check the document version of this publication:

• A submitted manuscript is the version of the article upon submission and before peer-review. There can be important differences between the submitted version and the official published version of record. People interested in the research are advised to contact the author for the final version of the publication, or visit the DOI to the publisher's website.
• The final author version and the galley proof are versions of the publication after peer review.
• The final published version features the final layout of the paper including the volume, issue and page numbers.

Link to publication

General rights
Copyright and moral rights for the publications made accessible in the public portal are retained by the authors and/or other copyright owners and it is a condition of accessing publications that users recognise and abide by the legal requirements associated with these rights.

• Users may download and print one copy of any publication from the public portal for the purpose of private study or research.
• You may not further distribute the material or use it for any profit-making activity or commercial gain
• You may freely distribute the URL identifying the publication in the public portal.

If the publication is distributed under the terms of Article 25fa of the Dutch Copyright Act, indicated by the "Taverne" license above, please follow below link for the End User Agreement:

www.tue.nl/taverne

Take down policy
If you believe that this document breaches copyright please contact us at:

openaccess@tue.nl

providing details and we will investigate your claim.

Download date: 04. Oct. 2023

PRELIMINARY REPORT ON

In-Duct and Radiation Matching Strategies

TURBONOISECFD WORKPACKAGE 2

DELIVERABLE D2.3

by

S.W. Rienstra (TUE) & Xin Zhang (ISVR)

March 2001

Contents

Part A:

The In-Duct Matching Problem

S.W. Rienstra
Eindhoven University of Technology
P.O.Box 513, 5600 MB Eindhoven, NL
February 22, 2001

Summary

The matching problem is considered across the interface between a region with CFD-type full Navier-Stokes modelling (the source region) and a region (duct) with an acoustic field with mean flow modelling. The discontinuous field cannot be avoided. Therefore a method is proposed, based on a modal representation of the acoustic field, to determine the field as well as possible by means of a least squares modification of a Galerkin-type mode matching.

1 Introduction

1.1 The CFD and acoustic zones and their interfaces

In the CFD regions (fig.1, or zones 4,6,7,15 in fig.2) the unsteady parts of all flow variables like pressure, velocity, density and possibly the thermodynamic variables are of the same order of magnitude as the steady (time-averaged) parts. In the acoustic regions (zones 1,3,5,8,9, 10,16,18 in fig.2) the unsteady components are small compared to the steady (mean) flow. Therefore, the way the CFD flow is determined is much different and usually numerically more advanced and calculation-intensive than the acoustic field.

Apart from that, the underlying models may vary considerably. The flow may be (Reynolds-averaged turbulent) viscous, isentropic, irrotational, cylindrical symmetric, of single frequency, etc.

Therefore, to translate the CFD results (pressure, velocity) into a form suitable for serving as a source in the acoustic problem is not straightforward.

1.2 Continuity of acoustic field

At the interfaces (see fig.2) we jump from model A (the full Navier-Stokes, say) into model B (inviscid flow with acoustic perturbations, say). The mean flow variables, that are consistent within model A, are almost certainly not consistent within model B, in other words: do not satisfy the equations. Therefore, some of the field variables (both of mean flow and perturbation) will have to be discontinuous at the interface. Any attempt to make more than one of the acoustic variables continuous has to be paid by a just as unphysical and artificial reflected field.

All this is an artefact of the fact that we change from one model to another and these reflections should be considered just as much of an error as the discontinuities. However, the CFD results are produced without taking into account any back-reaction, such that the field at the interface is as much as possible outgoing. Therefore, we should consider the possibility of minimizing both the reflections and the discontinuities.

As a result, it seems best to *define* somehow the field at the interface as unidirectionally outgoing. To achieve this, the equations should be solved at least locally near the interface such that incoming and outgoing waves can be separated. This may be approached in various ways. First is an acoustic analogy approach (FW-H, or Kirchhoff type) where the interface is suitably applied with flow sources [9, 8] and will be studied separately in part B of this document. The second route is the idea of local parabolic approximation or wave splitting [11, 10] and is most conveniently applied to a modal representation of the sound field, if available.

1.3 Reflection free boundary conditions

Ideally, the CFD flow is computed with reflection-free boundary conditions. To formulate such boundary conditions is a significant problem in its own right and an important part of the CFD calculations. Strictly speaking, it is separate from the matching problem and in practice it can only be achieved by manipulations, similar to the ones we are going to deal with here.

To eliminate false reflections from the interface in the CFD results, a CFD model A may at or near the interface be approximated by a simpler model $\widetilde{A}$ (usually one which is valid for inviscid linear perturbations and without the turbulence model included). This model can be solved analytically and the right and left running waves can then be separated (wave splitting).

In order to continue beyond the interface, in the acoustic region, with an acoustic model B, we will do something similar: we will try to continue the CFD field smoothly into the acoustic field of model B and to recognize the spurious reflected modes resulting from the jump between model A and B. So even

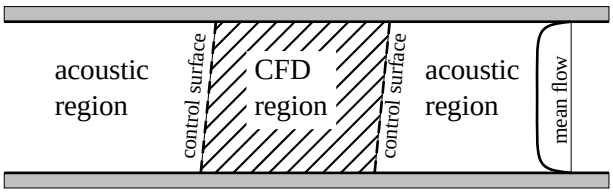

Figure 1: Sketch of CFD-region, acoustic region and interface.

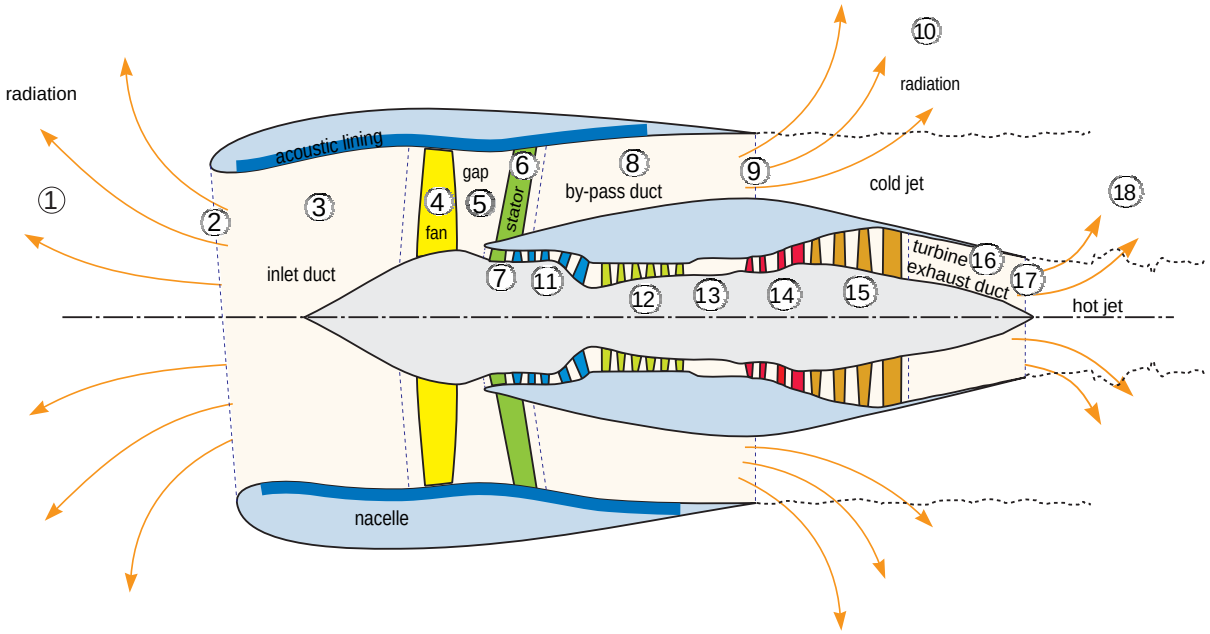

Figure 2: The zones

if the CFD results are ideal and reflection free in some sense, there will inevitably be false reflections from the non-ideal jump from model A to B.

Rather than assuming the CFD field to be reflection free and not even considering the possibility of a reflected field, it seems therefore a better strategy to include in the matching the detection of reflected modes. Of course, after detection these modes play no role in the acoustic problem and may be discarded.

1.4 The character of the jump

The ideal situation would be the control surface (between the CFD and the acoustic region) positioned far enough into the acoustic region, so that the acoustic equations are equivalent to the Navier-Stokes equations. We can then continue with either the given pressure or axial velocity distribution, p or v.

The real situation, however, is that the control surface is positioned as close to the CFD region as possible and we have to deal with a discontinuity in almost every mean flow variable. The acoustic field will then have to be discontinuous in some quantities. A question may be: which quantities should one make as continuous as possible.

As the CFD is nonlinear and the acoustic model is linear, the mean flow and acoustic mean flow will differ. In addition, the acoustic model is usually based on a simpler flow (irrotational, isentropic, inviscid, no swirl, etc.). Hence the “model-jump” is not always the same and the risk of an artificial source hidden in the interface will depend both on the mean flow and acoustic field model considered.

1.5 The mean flow

Another problem is that the CFD mean flow will have to be translated into the acoustic mean flow. We could define the CFD mean flow as the time-averaged CFD flow, while the unsteady part is defined as the acoustic and hydrodynamic perturbation. Note that (in the case of steady boundaries) this mean flow does not satisfy the steady version of the CFD problem (steady Euler, Navier Stokes, etc.) and that this perturbation does not exactly satisfy the linearized equations if the flow remains nonlinear.

As the various models are in general not equivalent, the mean flow obtained is still unable to satisfy the basic assumptions of the acoustic model and therefore the mean flow has to be stripped further to remove: swirl, entropy variations, vorticity and a strong radial component.

1.6 Modal decomposition

The wave splitting via modal decomposition is probably the best, or at least systematic, way to bring the CFD perturbations into an acoustic form. It hinges on the availability of generation of modes in cylindrical ducts with mean flow.

For plug flow the situation is fairly well established. Modes are formed by linear combinations of Bessel functions, while the eigenvalues are zeros of the derivatives. The modes are orthogonal, so there are no uniqueness problems. Hydrodynamic modes are pressureless (see below) which may confuse a description based on acoustic modes alone, but this seems to be a minor problem.

For parallel mean flow we have the Pridmore-Brown equation, for which the eigenvalue problem is more complicated, but it is soluable with the right numerical software; it may become problematic for higher frequencies. Modes are not orthogonal, so the amplitudes associated to a finite number are not unique. Hydrodynamic modes are also present.

For uniform mean flow with swirl, the mode problem [1, 2] becomes more and more complicated, especially if the swirl is arbitrary. Solid body rotation or free vortex swirl are relatively well studied. Little is known for more general parallel mean flow with swirl.

1.7 Hard wall

It is definitely easier to assume that the interface is positioned in a hard-walled section. This may not always be realistic, for example, the fan rotor section may be lined. However, most CFD routines seem not to be equipped with lined boundary conditions. Therefore, we will start by assuming hard walls.

2 Summary of equations for fluid motion

For future reference we will describe here a large number of possible acoustic models, systematically derived from the compressible Navier-Stokes equations, under the assumptions of absence of friction and thermal conduction and the fluid being a perfect gas. The flow is described by a steady mean flow and small perturbations, upon which linearization and Fourier time-analysis is possible. Further simplifications are considered based on axi-symmetric geometry and mean flow.

2.1 Conservation laws and constitutive equations

The original laws of mass, momentum and energy conservation, written in terms of pressure p, density ρ, velocity vector $\boldsymbol{v}$, scalar velocity $v = |\boldsymbol{v}|$, viscous stress tensor $\boldsymbol{\tau}$, internal energy density ϵ, total energy density e and heat flux vector $\boldsymbol{q}$, are given by

$$\begin{aligned}
\text{mass:} \quad & \tfrac{\partial}{\partial t}\rho \quad + \nabla\cdot(\rho\boldsymbol{v}) \quad = 0 && \text{(1a)}\\
\text{mom.:} \quad & \tfrac{\partial}{\partial t}(\rho\boldsymbol{v}) + \nabla\cdot(\rho\boldsymbol{v}\boldsymbol{v}) = -\nabla p + \nabla\cdot\boldsymbol{\tau} && \text{(1b)}\\
\text{energy:} \quad & \tfrac{\partial}{\partial t}(\rho e) + \nabla\cdot(\rho e\boldsymbol{v}) = -\nabla\cdot\boldsymbol{q} - \nabla\cdot(p\boldsymbol{v}) + \nabla\cdot(\boldsymbol{\tau}\boldsymbol{v}) && \text{(1c)}
\end{aligned}$$

while

$$e = \epsilon + \tfrac{1}{2}v^2. \tag{1d}$$

Depending of the application, it is often convenient to introduce enthalpy or heat function

$$h = \epsilon + \frac{p}{\rho}, \tag{2}$$

or entropy s and temperature T via the fundamental law of thermodynamics for a reversible process

$$T\,\mathrm{d}s = \mathrm{d}\epsilon + p\mathrm{d}\rho^{-1} = \mathrm{d}h - \rho^{-1}\mathrm{d}p. \tag{3}$$

With $\frac{\mathrm{d}}{\mathrm{d}t} = \frac{\partial}{\partial t} + \boldsymbol{v}\cdot\nabla$ for the convective derivative, the above conservation laws may be reduced to

$$\begin{aligned}
\text{mass:} \quad & \tfrac{\mathrm{d}}{\mathrm{d}t}\rho = -\rho\nabla\cdot\boldsymbol{v} && \text{(4a)}\\
\text{momentum:} \quad & \rho\tfrac{\mathrm{d}}{\mathrm{d}t}\boldsymbol{v} = -\nabla p + \nabla\cdot\boldsymbol{\tau} && \text{(4b)}\\
\text{energy :} \quad & \rho\tfrac{\mathrm{d}}{\mathrm{d}t}\epsilon = -\nabla\cdot\boldsymbol{q} - p\nabla\cdot\boldsymbol{v} + \boldsymbol{\tau}:\nabla\boldsymbol{v} && \text{(4c)}\\
& \rho\tfrac{\mathrm{d}}{\mathrm{d}t}h = \tfrac{\mathrm{d}}{\mathrm{d}t}p - \nabla\cdot\boldsymbol{q} + \boldsymbol{\tau}:\nabla\boldsymbol{v} && \text{(4d)}\\
& \rho T\tfrac{\mathrm{d}}{\mathrm{d}t}s = -\nabla\cdot\boldsymbol{q} + \boldsymbol{\tau}:\nabla\boldsymbol{v}. && \text{(4e)}
\end{aligned}$$

For acoustic applications the entropy form (4e) is the most convenient to use.

For an *ideal* gas we have the following relations

$$\begin{aligned}
p &= \rho\mathcal{R}T, && \text{(5a)}\\
\mathrm{d}\epsilon &= C_V\mathrm{d}T, && \text{(5b)}\\
\mathrm{d}h &= C_P\mathrm{d}T, && \text{(5c)}
\end{aligned}$$

where C_V is the heat capacity or specific heat at constant volume, C_P is the heat capacity or specific heat at constant pressure [12] and both C_V and C_P may be functions of T. $\mathcal{R}$ is the specific gas constant and γ the Poisson ratio, which are practically constant and given by (the figures refer to air)

$$\mathcal{R} = C_P - C_V = 286.73\ \mathrm{J/kg\,K}, \qquad \gamma = \frac{C_P}{C_V} = 1.402 \tag{6}$$

From equation (3) it then follows for an ideal gas that

$$\mathrm{d}s = C_V\frac{\mathrm{d}p}{p} - C_P\frac{\mathrm{d}\rho}{\rho} \tag{7}$$

while isentropic perturbations ($\mathrm{d}s = 0$), like sound, propagate with sound speed c given by the expression

$$c^2 = \left(\frac{\partial p}{\partial \rho}\right)_s = \frac{\gamma p}{\rho} = \gamma \mathcal{R} T. \tag{8}$$

In the case of a *perfect* gas, the specific heats are constant and we can integrate (apart from an immaterial integration constant) the equations (5) to obtain

$$\epsilon = C_V T, \tag{9a}$$
$$h = C_P T, \tag{9b}$$
$$s = C_V \log p - C_P \log \rho. \tag{9c}$$

2.2 In a rotating frame of reference

For axes, rotating steadily relative to the absolute frame of reference, we have to include fictitious body forces due to rotation. If the moving frame of reference is rotating with angular velocity $\boldsymbol{\Omega}$ and $\boldsymbol{x}$ is the relative position vector, the absolute velocity is given by $\boldsymbol{v}_{\text{abs}} = \boldsymbol{v} + \boldsymbol{\Omega}\times\boldsymbol{x}$ and the equations (1) take the form

$$\text{mass:} \quad \tfrac{\partial}{\partial t}\rho \quad + \nabla\cdot(\rho\boldsymbol{v}) \quad = 0 \tag{10a}$$
$$\text{mom.:} \quad \tfrac{\partial}{\partial t}(\rho\boldsymbol{v}) + \nabla\cdot(\rho\boldsymbol{v}\boldsymbol{v}) = -2\boldsymbol{\Omega}\times\boldsymbol{v} - \boldsymbol{\Omega}\times(\boldsymbol{\Omega}\times\boldsymbol{x}) - \nabla p + \nabla\cdot\boldsymbol{\tau} \tag{10b}$$
$$\text{energy:} \quad \tfrac{\partial}{\partial t}(\rho e) + \nabla\cdot(\rho e\boldsymbol{v}) = -\nabla\cdot\boldsymbol{q} - \nabla\cdot(p\boldsymbol{v}) + \nabla\cdot(\boldsymbol{\tau}\boldsymbol{v}) \tag{10c}$$

where

$$e = \epsilon + \tfrac{1}{2}\big(v^2 + |\boldsymbol{\Omega}|^2|\boldsymbol{x}|^2 - (\boldsymbol{\Omega}\cdot\boldsymbol{x})^2\big). \tag{10d}$$

If $\boldsymbol{\Omega} = \Omega\boldsymbol{e}_x$ and r is the radial coordinate in the cylindrical coordinate system (x, r, θ), this simplifies to

$$e = \epsilon + \tfrac{1}{2}v^2 + \tfrac{1}{2}\Omega^2 r^2. \tag{10e}$$

2.3 Acoustic applications

In the acoustic realm to be considered, the viscous or turbulent stress terms are assumed to play a role only within the source region, while any perturbation is assumed too fast to be affected by thermal conduction. Therefore, for the present applications of acoustic propagation we intend to ignore viscous shear stress ($\boldsymbol{\tau}$) and thermal conduction ($\boldsymbol{q}$), such that we have

$$\tfrac{\mathrm{d}}{\mathrm{d}t}\rho = -\rho\nabla\cdot\boldsymbol{v}, \tag{11a}$$
$$\rho\tfrac{\mathrm{d}}{\mathrm{d}t}\boldsymbol{v} = -\nabla p, \tag{11b}$$
$$\tfrac{\mathrm{d}}{\mathrm{d}t}s = 0. \tag{11c}$$

This means that entropy remains constant and thus $\mathrm{d}h = \rho^{-1}\mathrm{d}p$, along pathlines.

Furthermore, we will assume the gas to be perfect, with the following thermodynamical closure relations

$$s = C_V \log p - C_P \log \rho, \quad c^2 = \frac{\gamma p}{\rho}. \tag{11d}$$

2.4 Perturbations of a mean flow

When we have a steady mean flow with unsteady perturbations, given by

$$\boldsymbol{v} = \boldsymbol{V} + \boldsymbol{v}', \quad p = P + p', \quad \rho = D + \rho', \quad s = S + s' \tag{12}$$

and linearize for small amplitudes, we subsequently obtain for the mean flow

$$\nabla\cdot\big(D\boldsymbol{V}\big) = 0, \tag{13a}$$

$$D\big(\boldsymbol{V}\cdot\nabla\big)\boldsymbol{V} = -\nabla P, \tag{13b}$$

$$\big(\boldsymbol{V}\cdot\nabla\big)S = 0, \tag{13c}$$

with

$$S = C_V \log P - C_P \log D, \quad C^2 = \frac{\gamma P}{D} \tag{13d}$$

and the perturbations are governed by

$$\tfrac{\partial}{\partial t}\rho' + \nabla\cdot\big(\boldsymbol{V}\rho' + \boldsymbol{v}'D\big) = 0 \tag{14a}$$

$$D\big(\tfrac{\partial}{\partial t} + \boldsymbol{V}\cdot\nabla\big)\boldsymbol{v}' + D\big(\boldsymbol{v}'\cdot\nabla\big)\boldsymbol{V} + \rho'\big(\boldsymbol{V}\cdot\nabla\big)\boldsymbol{V} = -\nabla p' \tag{14b}$$

$$\big(\tfrac{\partial}{\partial t} + \boldsymbol{V}\cdot\nabla\big)s' + \boldsymbol{v}'\cdot\nabla S = 0 \tag{14c}$$

with

$$s' = \frac{C_V}{P}p' - \frac{C_P}{D}\rho', \quad c' = \tfrac{1}{2}C\Big(\frac{p'}{P} - \frac{\rho'}{D}\Big). \tag{14d}$$

The expression for c' usually serves no purpose in linear acoustics.

2.5 Bernoulli for the mean flow

Since S remains constant along streamlines, we can introduce the mean flow enthalpy H, with $\mathrm{d}H = D^{-1}\mathrm{d}P$. When we integrate the momentum equation (13b)

$$\boldsymbol{V}\cdot\nabla\boldsymbol{V} = \tfrac{1}{2}\nabla V^2 + (\nabla\times\boldsymbol{V})\times\boldsymbol{V} = -D^{-1}\nabla P = -\nabla H \tag{15}$$

along a streamline, noting that $(\nabla\times\boldsymbol{V})\times\boldsymbol{V}$ is orthogonal to $\boldsymbol{V}$ and therefore to the streamline, we obtain for the mean flow a form of Bernoulli's equation as follows:

$$\tfrac{1}{2}V^2 + H = \text{constant along a streamline.} \tag{16}$$

2.6 Homentropic mean flow

If the mean flow is homentropic ($S =$ constant), for example when P and D are constant, the perturbations are isentropic along streamlines and the pressure and density are related by

$$\big(\tfrac{\partial}{\partial t} + \boldsymbol{V}\cdot\nabla\big)p' = C^2\big(\tfrac{\partial}{\partial t} + \boldsymbol{V}\cdot\nabla\big)\rho' \tag{17}$$

2.7 Isentropic perturbations

If the perturbations are entirely isentropic ($s' \equiv 0$), for example when $\boldsymbol{V} = 0$ and $S =$ constant, the pressure and density perturbations are related by the usual expression

$$p' = C^2 \rho'. \tag{18}$$

2.8 Time harmonic

When the perturbations are time-harmonic, given by (note the $+\mathrm{i}\omega t$ convention)

$$\boldsymbol{v}' = \mathrm{Re}(\boldsymbol{v}\, \mathrm{e}^{\mathrm{i}\omega t}),\ \ p' = \mathrm{Re}(p\, \mathrm{e}^{\mathrm{i}\omega t}),\ \ \rho' = \mathrm{Re}(\rho\, \mathrm{e}^{\mathrm{i}\omega t}),\ \ s' = \mathrm{Re}(s\, \mathrm{e}^{\mathrm{i}\omega t}) \tag{19}$$

(where we ignore the prime from here on), we then find in the usual complex notation

$$\mathrm{i}\omega\rho + \nabla\cdot\big(\boldsymbol{V}\rho + \boldsymbol{v}D\big) = 0, \tag{20a}$$

$$D\big(\mathrm{i}\omega + \boldsymbol{V}\cdot\nabla\big)\boldsymbol{v} + D\big(\boldsymbol{v}\cdot\nabla\big)\boldsymbol{V} + \rho\big(\boldsymbol{V}\cdot\nabla\big)\boldsymbol{V} = -\nabla p, \tag{20b}$$

$$\big(\mathrm{i}\omega + \boldsymbol{V}\cdot\nabla\big)s + \boldsymbol{v}\cdot\nabla S = 0, \tag{20c}$$

$$s = \frac{C_V}{P}p - \frac{C_P}{D}\rho. \tag{20d}$$

Note that further systematic simplifications are possible if we take into account the fact that in an engine duct the axial velocity dominates, while at the same time axial variation of the mean flow variables is relatively slow due to the (necessarily!) slowly varying geometry.

2.9 Irrotational isentropic flow

When the flow is irrotational and isentropic everywhere (homentropic), for example in the inlet, or when we assume this condition for reasons of computational efficiency, for example in the by-pass duct, we can introduce a potential ϕ for the velocity, where $\boldsymbol{v} = \nabla\phi$ and express p as a function of ρ only. We can then integrate the momentum equation and obtain the important simplification

$$\frac{\partial}{\partial t}\phi + \tfrac{1}{2}\big|\nabla\phi\big|^2 + \frac{c^2}{\gamma - 1} = \text{constant}, \qquad \frac{p}{\rho^\gamma} = \text{constant} \tag{21}$$

that produces for the mean flow and harmonic perturbation (introduce $\phi = \Phi + \phi' = \Phi + \phi\, \mathrm{e}^{\mathrm{i}\omega t}$) the following equations

$$\nabla\cdot\big(D\nabla\Phi\big) = 0, \quad \tfrac{1}{2}\big|\nabla\Phi\big|^2 + \frac{C^2}{\gamma - 1} = \text{constant}, \quad \frac{P}{D^\gamma} = \text{constant} \tag{22a}$$

$$\mathrm{i}\omega\rho + \nabla\cdot\big(\rho\nabla\Phi + D\nabla\phi\big) = 0, \quad D\big(\mathrm{i}\omega\phi + \nabla\Phi\cdot\nabla\phi\big) + p = 0, \quad p = C^2\rho \tag{22b}$$

The entropy equation becomes a superfluous identity.

2.10 Circular symmetric geometry

To make further progress, we assume a geometry that in the immediate neighbourhood of the interface is equal to a hollow or annular cylinder of solid walls, while the mean flow is taken to be circular symmetric and axially constant. In that case the mean flow cannot have a non-zero radial component and is a function of the radial coordinate r only. With axial component U (in x-direction) and circumferential component W (in θ-direction) the mean flow variables become

$$\boldsymbol{V} = U(r)\boldsymbol{e}_x + W(r)\boldsymbol{e}_\theta, \quad D = D(r), \quad P = P(r), \qquad S = S(r), \tag{23}$$

and the pressure is independent of x (whence the pressure gradient vanishes) because the flow is parallel and frictionless.

All mean flow equations are now identically satisfied, except for

$$\frac{D}{r}W^2 = \frac{\partial P}{\partial r}, \tag{24}$$

and so any mean flow profiles U, W, D, P, S may be assumed, as long as they satisfy the two consistency relations

$$P = \int^r \frac{D}{r}W^2 \,\mathrm{d}r', \quad S = C_V \log P - C_P \log D. \tag{25}$$

Without swirl (*i.e.* $W = 0$), P is a constant, while D may vary in r if S does. A homentropic flow without swirl implies that D is a constant.

If the flow is irrotational and we want to describe it by means of a velocity potential, the most general form of the mean flow potential Φ is

$$\Phi = Ux + \Gamma\theta, \quad \text{with } \boldsymbol{V} = U\boldsymbol{e}_x + \frac{\Gamma}{r}\boldsymbol{e}_\theta \tag{26}$$

where U and Γ are constants. If the flow is also homentropic ($S = S_0 =$ constant), the general form of the pressure and density is

$$P = \left(P_0 - \frac{\gamma - 1}{2\gamma}\,\mathrm{e}^{-S_0/C_P}\,\frac{\Gamma^2}{r^2}\right)^{\frac{\gamma}{\gamma-1}}, \qquad D = P^{1/\gamma}\,\mathrm{e}^{-S_0/C_P} \tag{27}$$

where P_0 is a constant.

An important special case is that of uniform flow with $\Gamma = 0$ and P and D constant.

2.11 Types of swirl

Typically, the following cases occur in a turbomachine duct

- In the inlet, the mean flow is nearly uniform and irrotational and typically we have a thin boundary layer and a circumferential velocity, or swirl, given by

$$W \simeq 0 \tag{28a}$$

- In the compressor stages, the pressure increases quickly and the boundary layer is most probably thin.

- In the compressor, behind a stator or guide vanes and before a rotor, the mean flow is close to that of a rigid body rotation and the circumferential velocity is typically

$$W \simeq \Omega r \tag{28b}$$

- In the compressor, behind a rotor and before a stator or guide vanes, the mean flow also contains rotation, for example in the form of a free axial vortex and the circumferential velocity is typically

$$W \simeq \Omega r + \frac{\Gamma}{r} \tag{28c}$$

- Behind the compressor, for example in the by-pass duct, the swirl W is again small, but the boundary layer may be significant acoustically (refraction).

We will not assume here any further mean flow profile. It should, however, be noted that we will assume a discrete spectrum for the modal expansion to be introduced below ("normal modes approach"). Although the matter is not completely settled yet, there is strong evidence in the literature that a discrete set of modes is not a complete basis of the solution space of the present equations considered if the mean flow profile is arbitrary. At least in principle, care should be taken when the profile allows critical layers (the radial position where the convected derivative $(\mathrm{i}\omega + \boldsymbol{V}\cdot\nabla)$ vanishes). Only if the mean flow is simple enough (like the above cases) does the modal spectrum seems to be discrete everywhere.

3 Acoustic equations with circular symmetric geometry

The acoustic equations, corresponding with the circular symmetric mean flow introduced in section 2.10, are as follows. When we introduce for the perturbation velocity vector

$$\boldsymbol{v} = u\boldsymbol{e}_x + v\boldsymbol{e}_r + w\boldsymbol{e}_\theta \tag{29}$$

the harmonic perturbation equations are written out in full (a prime denotes a derivative to r of the mean flow variable) in the subsections below*.

*Recall the following identities in cylindrical co-ordinates for vector fields $\boldsymbol{v}$ and $\boldsymbol{V}$ and a scalar ϕ

$$\begin{aligned}
\nabla\cdot\boldsymbol{v} &= \tfrac{\partial}{\partial x}u + \tfrac{\partial}{\partial r}v + \tfrac{1}{r}v + \tfrac{1}{r}\tfrac{\partial}{\partial\theta}w \\
\boldsymbol{V}\cdot\nabla\boldsymbol{v} &= \big(U\tfrac{\partial}{\partial x}u + V\tfrac{\partial}{\partial r}u + \frac{1}{r}W\tfrac{\partial}{\partial\theta}u\big)\boldsymbol{e}_x + \big(U\tfrac{\partial}{\partial x}v + V\tfrac{\partial}{\partial r}v + \tfrac{1}{r}W\big(\tfrac{\partial}{\partial\theta}v - w\big)\big)\boldsymbol{e}_r \\
&\qquad + \big(U\tfrac{\partial}{\partial x}w + V\tfrac{\partial}{\partial r}w + \tfrac{1}{r}W(\tfrac{\partial}{\partial\theta}w + v)\big)\boldsymbol{e}_\theta \\
\nabla\times\boldsymbol{v} &= \big(\tfrac{\partial}{\partial r}w + \tfrac{1}{r}w - \tfrac{1}{r}\tfrac{\partial}{\partial\theta}v\big)\boldsymbol{e}_x + \big(\tfrac{1}{r}\tfrac{\partial}{\partial\theta}u - \tfrac{\partial}{\partial x}w\big)\boldsymbol{e}_r + \big(\tfrac{\partial}{\partial x}v - \tfrac{\partial}{\partial r}u\big)\boldsymbol{e}_\theta \\
\nabla\phi &= \tfrac{\partial}{\partial r}\phi\boldsymbol{e}_r + \tfrac{1}{r}\tfrac{\partial}{\partial\theta}\phi\boldsymbol{e}_\theta + \tfrac{\partial}{\partial x}\phi\boldsymbol{e}_x.
\end{aligned}$$

3.1 With swirl and variable entropy

$$\Big(\mathrm{i}\omega + U\frac{\partial}{\partial x} + \frac{W}{r}\frac{\partial}{\partial \theta}\Big)\rho + D\Big(\frac{\partial u}{\partial x} + \frac{1}{r}\frac{\partial}{\partial r}(rv) + \frac{1}{r}\frac{\partial w}{\partial \theta}\Big) + D'v = 0 \tag{30a}$$

$$D\Big(\mathrm{i}\omega + U\frac{\partial}{\partial x} + \frac{W}{r}\frac{\partial}{\partial \theta}\Big)u + DU'v + \frac{\partial p}{\partial x} = 0 \tag{30b}$$

$$D\Big(\mathrm{i}\omega + U\frac{\partial}{\partial x} + \frac{W}{r}\frac{\partial}{\partial \theta}\Big)v - \frac{2DW}{r}w - \frac{W^2}{r}\rho + \frac{\partial p}{\partial r} = 0 \tag{30c}$$

$$D\Big(\mathrm{i}\omega + U\frac{\partial}{\partial x} + \frac{W}{r}\frac{\partial}{\partial \theta}\Big)w + \frac{DW}{r}v + DW'v + \frac{1}{r}\frac{\partial p}{\partial \theta} = 0 \tag{30d}$$

$$\Big(\mathrm{i}\omega + U\frac{\partial}{\partial x} + \frac{W}{r}\frac{\partial}{\partial \theta}\Big)s + S'v = 0 \tag{30e}$$

By using relation (20d) between s, p and ρ and equation (30a), s can be eliminated and equation (30e) replaced by

$$\Big(\mathrm{i}\omega + U\frac{\partial}{\partial x} + \frac{W}{r}\frac{\partial}{\partial \theta}\Big)\big(p - C^2\rho\big) + \Big(\frac{DW^2}{r} - C^2D'\Big)v = 0 \tag{30f}$$

3.2 Without swirl and variable entropy

Without swirl the harmonic perturbation equations are

$$\Big(\mathrm{i}\omega + U\frac{\partial}{\partial x}\Big)\rho + D\Big(\frac{\partial u}{\partial x} + \frac{1}{r}\frac{\partial}{\partial r}(rv) + \frac{1}{r}\frac{\partial w}{\partial \theta}\Big) + D'v = 0 \tag{31a}$$

$$D\Big(\mathrm{i}\omega + U\frac{\partial}{\partial x}\Big)u + DU'v + \frac{\partial p}{\partial x} = 0 \tag{31b}$$

$$D\Big(\mathrm{i}\omega + U\frac{\partial}{\partial x}\Big)v + \frac{\partial p}{\partial r} = 0 \tag{31c}$$

$$D\Big(\mathrm{i}\omega + U\frac{\partial}{\partial x}\Big)w + \frac{1}{r}\frac{\partial p}{\partial \theta} = 0 \tag{31d}$$

$$\Big(\mathrm{i}\omega + U\frac{\partial}{\partial x}\Big)\big(p - C^2\rho\big) - C^2D'v = 0 \tag{31e}$$

3.3 Homentropic without swirl

Without swirl and entropy variations the harmonic perturbation equations are

$$\Big(\mathrm{i}\omega + U\frac{\partial}{\partial x}\Big)\rho + D\Big(\frac{\partial u}{\partial x} + \frac{1}{r}\frac{\partial}{\partial r}(rv) + \frac{1}{r}\frac{\partial w}{\partial \theta}\Big) = 0 \tag{32a}$$

$$D\Big(\mathrm{i}\omega + U\frac{\partial}{\partial x}\Big)u + DU'v + \frac{\partial p}{\partial x} = 0 \tag{32b}$$

$$D\Big(\mathrm{i}\omega + U\frac{\partial}{\partial x}\Big)v + \frac{\partial p}{\partial r} = 0 \tag{32c}$$

$$D\Big(\mathrm{i}\omega + U\frac{\partial}{\partial x}\Big)w + \frac{1}{r}\frac{\partial p}{\partial \theta} = 0 \tag{32d}$$

$$p - C^2\rho = 0 \tag{32e}$$

3.4 Irrotational homentropic flow

When the flow is irrotational and homentropic, we can introduce a potential in the form of equation (26) and integrate the momentum equation (22). P and D are in the form of equation (27), while U and Γ are constants. The result is the expressions:

$$\Big(\mathrm{i}\omega + U\frac{\partial}{\partial x} + \frac{\Gamma}{r^2}\frac{\partial}{\partial\theta}\Big)\rho + D\Big(\frac{\partial^2\phi}{\partial x^2} + \frac{1}{r}\frac{\partial}{\partial r}\big(r\frac{\partial\phi}{\partial r}\big) + \frac{1}{r^2}\frac{\partial^2\phi}{\partial\theta^2}\Big) + D'\frac{\partial\phi}{\partial r} = 0 \tag{33a}$$

$$D\Big(\mathrm{i}\omega + U\frac{\partial}{\partial x} + \frac{\Gamma}{r^2}\frac{\partial}{\partial\theta}\Big)\phi + p = 0 \tag{33b}$$

$$p - C^2\rho = 0 \tag{33c}$$

3.5 Uniform mean flow

The simplest, but therefore the most important configuration is the one with a uniform mean flow. Note that this does **not** exactly imply irrotational and isentropic perturbations.

Axial mean velocity U, mean pressure P, density D and sound speed C are constants, so we have

$$\Big(\mathrm{i}\omega + U\frac{\partial}{\partial x}\Big)\rho + D\Big(\frac{\partial u}{\partial x} + \frac{1}{r}\frac{\partial}{\partial r}(rv) + \frac{1}{r}\frac{\partial w}{\partial\theta}\Big) = 0, \tag{34a}$$

$$D\Big(\mathrm{i}\omega + U\frac{\partial}{\partial x}\Big)u + \frac{\partial p}{\partial x} = 0, \tag{34b}$$

$$D\Big(\mathrm{i}\omega + U\frac{\partial}{\partial x}\Big)v + \frac{\partial p}{\partial r} = 0, \tag{34c}$$

$$D\Big(\mathrm{i}\omega + U\frac{\partial}{\partial x}\Big)w + \frac{1}{r}\frac{\partial p}{\partial\theta} = 0, \tag{34d}$$

$$\Big(\mathrm{i}\omega + U\frac{\partial}{\partial x}\Big)\big(p - C^2\rho\big) = 0. \tag{34e}$$

We then split the perturbation velocity into a vortical part and an irrotational part by introducing the vector potential (stream function) $\boldsymbol{\Psi}$ and scalar potential ϕ as follows (see the footnote on page 14)

$$\boldsymbol{v} = \nabla\times\boldsymbol{\Psi} + \nabla\phi, \tag{35}$$

If desired, the arbitrariness in $\boldsymbol{\Psi}$ (we may add any ∇f, since $\nabla\times\nabla f \equiv 0$) may be removed by adding the gauge condition $\nabla\cdot\boldsymbol{\Psi} = 0$, such that the vorticity is given by

$$\boldsymbol{\xi} = \nabla\times\boldsymbol{v} = \nabla(\nabla\cdot\boldsymbol{\Psi}) - \nabla^2\boldsymbol{\Psi} = -\nabla^2\boldsymbol{\Psi}. \tag{36}$$

Since the divergence of a curl is zero, $\nabla\cdot\boldsymbol{v} = \nabla\cdot(\nabla\times\boldsymbol{\Psi} + \nabla\phi) = \nabla^2\phi$ and equation (34a) becomes

$$\Big(\mathrm{i}\omega + U\frac{\partial}{\partial x}\Big)\rho + D\nabla^2\phi = 0 \tag{37}$$

From the equations (34b-d), given in vector form by

$$D\Big(\mathrm{i}\omega + U\frac{\partial}{\partial x}\Big)\big(\nabla\times\boldsymbol{\Psi} + \nabla\phi\big) + \nabla p = 0, \tag{38}$$

we readily see that by taking the divergence of equation (38) and using equations (34e) and (37), we can eliminate ϕ and ρ to obtain the convected reduced wave equation for the pressure

$$C^2\nabla^2 p - \Big(\mathrm{i}\omega + U\frac{\partial}{\partial x}\Big)^2 p = 0. \tag{39}$$

(Note that we did not assume the isentropy relation $p = C^2\rho$.) With some care, especially taking due notice of the singular edge behaviour, this equation may be transformed to the ordinary reduced wave equation by allowing

$$\begin{aligned} p(x, r, \theta; \omega) &= \widetilde{p}(X, r, \theta; \Omega)\exp(\mathrm{i}\tfrac{\Omega M}{C}X), \\ \text{where} \quad x = \beta X,\ \omega &= \beta\Omega,\ M = \frac{U}{C},\ \beta = \sqrt{1-M^2}. \end{aligned} \tag{40}$$

In addition, by taking the curl of equations 34(b-d) we can eliminate p and ϕ to produce an equation for the vorticity:

$$-\Big(\mathrm{i}\omega + U\frac{\partial}{\partial x}\Big)\nabla^2\boldsymbol{\Psi} = \Big(\mathrm{i}\omega + U\frac{\partial}{\partial x}\Big)\boldsymbol{\xi} = 0. \tag{41}$$

Summarizing, we found a convected wave equation (39) for the pressure, and equations that describe simple mean flow convection for the entropy (34e) and for the vorticity (41). These three equations are (in this uniform flow case) completely independent and therefore describe independent quantities. Since the velocity fluctuations are determined by a sum of acoustic contributions (connected to p) and vortical contributions (connected to $\boldsymbol{\xi}$), any acoustic information from the velocity alone is impossible if the flow is not irrotational (as in the by-pass duct, or anywhere behind a rotor or stator).

In such a case information on the direction of the wave might better be found from $\frac{\partial}{\partial x}p$, the axial derivative of the pressure. This aspect will have to be carefully taken into account in the issue of matching to be considered below.

4 Interface and boundary conditions

4.1 Hard wall conditions

At the solid walls at $r = R_1$ and $r = R_2$ the radial component of the velocity vanishes

$$v(x, r, \theta) = 0 \ \text{ at } \ r = R_1,\ r = R_2. \tag{42}$$

4.2 The interface

To allow more general configurations (for example, with swept vanes or blades), the interface between the source region and the rest of the duct is assumed to be given by the conical surface

$$x_i(r) = x_0 + \lambda r. \tag{43}$$

At this control surface the field $\boldsymbol{v}$, p, ρ, s is given. If we take the more important ones (but this is a matter of taste), they may be described by

$$p(x_i, r, \theta) = \mathcal{P}(r, \theta), \quad u(x_i, r, \theta) = \mathcal{U}(r, \theta), \quad s(x_i, r, \theta) = \mathcal{S}(r, \theta), \tag{44}$$

and as they are the product of another model (*e.g.* , CFD based on RANS), it is almost inevitable and that they are not consistent with the present model.

We have the following options.

(i) Assume that one of the field variables (for example pressure) should be continuous, *i.e.* prescribed by the source region at the interface. The other field variables of the resulting field will be discontinuous at the interface. In this case it is not possible to include all incoming and outgoing waves because the resulting field would radiate symmetrically away from the interface and comprise of about as many incoming waves as outgoing waves. Therefore, the amplitudes would be about half of what they should be.

Therefore, with this option it is not only natural but also necessary to assume beforehand that the incoming waves are absent.

(ii) Do the same as under (i) for any of the field variables and take the average.

(iii) Rather than taking the average, we formulate a least squares problem, such that the discontinuity is evenly distributed over the chosen field variables.

(iv) We could try to take into account the fact that the CFD interface boundary condition is not perfect and that the produced field is not yet free of spurious reflections. In this case we could include, on either side of the interface, both reflected (incoming) and transmitted (outgoing) waves. On physical grounds (see above, option i), we then know that we will in turn require continuity of at least 2 variables.

The usual direct approach, aiming at continuous pressure and axial velocity, is rather complicated and requires a careful bookkeeping of matrices and submatrices.

The least squares method of option (iii), however, appears to include very easily waves in both directions. Therefore, we propose here a more general (new?) approach, to minimize the discontinuities over the most important variables in a suitable least squares sense. In the case of two variables, the obtained minimum should be nearly equivalent to the direct method, while in the case of more variables the error is spread.

Note that in option (iv) the reflections are a *mix* of the effects of the imperfect CFD radiation condition and the inherent modelling discontinuity. As we argued before, there is absolutely no reason to include reflections due to the modelling jump. Therefore, this option is only useful if this jump is small and the acoustic model is *practically equivalent* to the linearized version of the CFD model.

We do not intend to consider the possibility that (in option iv) the spurious reflections are (iteratively) coupled back to the CFD calculations, such that these reflections are made to vanish. This is practically only possible if both CFD and acoustic calculations are run in parallel on the same computer.

Therefore, one might argue that there is no real need to include reflected waves and that it is sufficient to apply the method to the outgoing waves only. Although this is true in principle, there are still a few good reasons to at least investigate the possibility. (1) As we will see, the amount of work and programming is practically the same for option (iii) and (iv). (2) The filtering of false reflections would have been the final postprocessing of the CFD calculations anyway and if the acoustic model is not simpler than the reduced CFD model "$\widetilde{A}$" (see section 1.3), it is just as efficient to do it here. (3) The amount of reflection is a possible measure of the interface mismatch, which may be a useful diagnostic quantity for later analysis.

Option (i) is clearly the simplest one and we should certainly start with it, for example with the pressure. Then we should consider (ii) and repeat the manipulations with the axial velocity and entropy, to see if the resulting fields are reasonably similar, so that a simple average can be regarded as satisfactory.

The method, however, which eventually is likely to be the preferred one, is (iii) or (iv), since the amount of programming and calculation is only slightly more than with (ii).

5 Circumferential Fourier decomposition

In view of the circumferential periodicity of the solution, the dependent variables can be written as a Fourier series in θ. Because of the linearity and θ-independence of the equations, the problem can be solved per Fourier mode. Here we have

$$\boldsymbol{v} = \sum_{m=-\infty}^{\infty} \boldsymbol{v}_m(x,r)\,\mathrm{e}^{-\mathrm{i}m\theta}, \quad p = \sum_{m=-\infty}^{\infty} p_m(x,r)\,\mathrm{e}^{-\mathrm{i}m\theta}, \quad \rho = \sum_{m=-\infty}^{\infty} \rho_m(x,r)\,\mathrm{e}^{-\mathrm{i}m\theta}, \tag{45}$$

together with

$$\mathcal{U} = \sum_{m=-\infty}^{\infty} \mathcal{U}_m(r)\,\mathrm{e}^{-\mathrm{i}m\theta}, \quad \mathcal{P} = \sum_{m=-\infty}^{\infty} \mathcal{P}_m(r)\,\mathrm{e}^{-\mathrm{i}m\theta}, \quad \mathcal{S} = \sum_{m=-\infty}^{\infty} \mathcal{S}_m(r)\,\mathrm{e}^{-\mathrm{i}m\theta}\,. \tag{46}$$

The equations for each case reduce to:

5.1 With swirl and variable entropy

$$\Big(\mathrm{i}\omega + U\frac{\partial}{\partial x} - \frac{\mathrm{i}mW}{r}\Big)\rho_m + D\Big(\frac{\partial u_m}{\partial x} + \frac{1}{r}\frac{\partial}{\partial r}(r v_m) - \frac{\mathrm{i}m}{r}w_m\Big) + D' v_m = 0 \tag{47a}$$

$$D\Big(\mathrm{i}\omega + U\frac{\partial}{\partial x} - \frac{\mathrm{i}mW}{r}\Big)u_m + DU' v_m + \frac{\partial p_m}{\partial x} = 0 \tag{47b}$$

$$D\Big(\mathrm{i}\omega + U\frac{\partial}{\partial x} - \frac{\mathrm{i}mW}{r}\Big)v_m - \frac{2DW}{r}w_m - \frac{W^2}{r}\rho_m + \frac{\partial p_m}{\partial r} = 0 \tag{47c}$$

$$D\Big(\mathrm{i}\omega + U\frac{\partial}{\partial x} - \frac{\mathrm{i}mW}{r}\Big)w_m + \frac{DW}{r}v_m + DW' v_m - \frac{\mathrm{i}m}{r}p_m = 0 \tag{47d}$$

$$\Big(\mathrm{i}\omega + U\frac{\partial}{\partial x} - \frac{\mathrm{i}mW}{r}\Big)\big(p_m - C^2\rho_m\big) + \Big(\frac{DW^2}{r} - C^2 D'\Big)v_m = 0 \tag{47e}$$

5.2 Without swirl and variable entropy

$$\Big(\mathrm{i}\omega + U\frac{\partial}{\partial x}\Big)\rho_m + D\Big(\frac{\partial u_m}{\partial x} + \frac{1}{r}\frac{\partial}{\partial r}(r v_m) - \frac{\mathrm{i}m}{r}w_m\Big) + D' v_m = 0 \tag{48a}$$

$$D\Big(\mathrm{i}\omega + U\frac{\partial}{\partial x}\Big)u_m + DU' v_m + \frac{\partial p_m}{\partial x} = 0 \tag{48b}$$

$$D\Big(\mathrm{i}\omega + U\frac{\partial}{\partial x}\Big)v_m + \frac{\partial p_m}{\partial r} = 0 \tag{48c}$$

$$D\Big(\mathrm{i}\omega + U\frac{\partial}{\partial x}\Big)w_m - \frac{\mathrm{i}m}{r}p_m = 0 \tag{48d}$$

$$\Big(\mathrm{i}\omega + U\frac{\partial}{\partial x}\Big)\big(p_m - C^2\rho_m\big) - C^2 D' v_m = 0 \tag{48e}$$

5.3 Homentropic without swirl

$$\Big(\mathrm{i}\omega + U\frac{\partial}{\partial x}\Big)\rho_m + D\Big(\frac{\partial u_m}{\partial x} + \frac{1}{r}\frac{\partial}{\partial r}(r v_m) - \frac{\mathrm{i}m}{r}w_m\Big) = 0 \tag{49a}$$

$$D\Big(\mathrm{i}\omega + U\frac{\partial}{\partial x}\Big)u_m + DU' v_m + \frac{\partial p_m}{\partial x} = 0 \tag{49b}$$

$$D\Big(\mathrm{i}\omega + U\frac{\partial}{\partial x}\Big)v_m + \frac{\partial p_m}{\partial r} = 0 \tag{49c}$$

$$D\Big(\mathrm{i}\omega + U\frac{\partial}{\partial x}\Big)w_m - \frac{\mathrm{i}m}{r}p_m = 0 \tag{49d}$$

$$p_m - C^2\rho_m = 0 \tag{49e}$$

5.4 Irrotational homentropic flow

$$\Big(\mathrm{i}\omega + U\frac{\partial}{\partial x} - \frac{\mathrm{i}m\Gamma}{r^2}\Big)\rho + D\Big(\frac{\partial^2\phi}{\partial x^2} + \frac{1}{r}\frac{\partial}{\partial r}\big(r\frac{\partial\phi}{\partial r}\big) - \frac{m^2}{r^2}\phi\Big) + D'\frac{\partial\phi}{\partial r} = 0 \tag{50a}$$

$$D\Big(\mathrm{i}\omega + U\frac{\partial}{\partial x} - \frac{\mathrm{i}m\Gamma}{r^2}\Big)\phi + p = 0 \tag{50b}$$

$$p - C^2\rho = 0 \tag{50c}$$

5.5 Uniform mean flow with irrotational isentropic perturbations

$$\Big(\mathrm{i}\omega + U\frac{\partial}{\partial x}\Big)\rho + D\Big(\frac{\partial^2\phi}{\partial x^2} + \frac{1}{r}\frac{\partial}{\partial r}\big(r\frac{\partial\phi}{\partial r}\big) - \frac{m^2}{r^2}\phi\Big) = 0 \tag{51a}$$

$$D\Big(\mathrm{i}\omega + U\frac{\partial}{\partial x}\Big)\phi + p = 0 \tag{51b}$$

$$p - C^2\rho = 0 \tag{51c}$$

6 Normal modes

In order to solve our present matching problem, we need to be able to distinguish incoming and outgoing (left and right running) waves. We do this by solving the above equations, assuming that they represent the field locally near the interface.

A general way to solve the equations, which are still partial differential equations in r and x, involves a Fourier transformation in x of the form

$$f(x,r) = \int_{-\infty}^{\infty} \hat{f}(r;\kappa)\, \mathrm{e}^{-\mathrm{i}\kappa x}\, \mathrm{d}\kappa \tag{52}$$

The resulting equations to be solved then become just ordinary differential equations in r. It will appear that the Fourier transformed solution has an infinite number of poles in the complex axial wave number plane, corresponding to the duct modes. If the Fourier transformed solution is meromorphic (analytic except for isolated poles $\kappa = \kappa_\mu$), the inverse transform can be evaluated and the solution in x-space can be written as an infinite modal sum. This appears to be the case if the mean flow is sufficiently simple (uniform, etc.). Symbolically, this is represented as

$$f(x,r) = \sum_{\mu=1}^{\infty} F_\mu^+(r)\, \mathrm{e}^{-\mathrm{i}\kappa_\mu^+ x} + \sum_{\mu=1}^{\infty} F_\mu^-(r)\, \mathrm{e}^{-\mathrm{i}\kappa_\mu^- x} \tag{53}$$

where the modal wave numbers κ_μ^+ and κ_μ^- correspond to right running and left running modes respectively.

In general, the Fourier transformed solution is not meromorphic and the solution has to be described by a modal sum plus an integral over the continuous part of the wave number spectrum. For example,

$$f(x,r) = \sum_{\mu=1}^{\infty} F_\mu^+(r)\, \mathrm{e}^{-\mathrm{i}\kappa_\mu^+ x} + \sum_{\mu=1}^{\infty} F_\mu^-(r)\, \mathrm{e}^{-\mathrm{i}\kappa_\mu^- x} + \int_{\mathcal{C}} \hat{f}(r;\kappa)\, \mathrm{e}^{-\mathrm{i}\kappa x}\, \mathrm{d}\kappa \tag{54}$$

Usually, this supplementary part seems to be of minor importance acoustically, as it refers mainly to hydrodynamic type of perturbations. Furthermore, it is also computationally very inconvenient. Therefore, we will ignore it here altogether and assume solutions of the form are just

$$\boldsymbol{v}_m = \sum_{\mu=-\infty}^{\infty} \boldsymbol{v}_{m\mu}(r)\, \mathrm{e}^{-\mathrm{i}\kappa_{m\mu} x}, \quad p_m = \sum_{\mu=-\infty}^{\infty} p_{m\mu}(r)\, \mathrm{e}^{-\mathrm{i}\kappa_{m\mu} x}, \quad s_m = \sum_{\mu=-\infty}^{\infty} s_{m\mu}(r)\, \mathrm{e}^{-\mathrm{i}\kappa_{m\mu} x} \tag{55}$$

(the distinction between left and right running will be made later) leading to the following reduced sets of equations. Introduce for national convenience

$$\Omega_{m\mu} = \omega - \kappa_{m\mu} U, \quad \Omega_{m\mu}^{(W)} = \omega - \kappa_{m\mu} U - \frac{mW}{r}, \quad \Omega_{m\mu}^{(\Gamma)} = \omega - \kappa_{m\mu} U - \frac{m\Gamma}{r^2}. \tag{56}$$

6.1 With swirl and variable entropy

$$\mathrm{i}\Omega^{(W)}_{m\mu}\rho_{m\mu} + D\Big(-\mathrm{i}\kappa_{m\mu}u_{m\mu} + \frac{1}{r}\frac{\partial}{\partial r}(r v_{m\mu}) - \frac{\mathrm{i}m}{r}w_{m\mu}\Big) + D' v_{m\mu} = 0 \tag{57a}$$

$$\mathrm{i}D\Omega^{(W)}_{m\mu}u_{m\mu} + DU' v_{m\mu} - \mathrm{i}\kappa_{m\mu}p_{m\mu} = 0 \tag{57b}$$

$$\mathrm{i}D\Omega^{(W)}_{m\mu}v_{m\mu} - \frac{2DW}{r}w_{m\mu} - \frac{W^2}{r}\rho_{m\mu} + \frac{\partial p_{m\mu}}{\partial r} = 0 \tag{57c}$$

$$\mathrm{i}D\Omega^{(W)}_{m\mu}w_{m\mu} + \frac{DW}{r}v_{m\mu} + DW' v_{m\mu} - \frac{\mathrm{i}m}{r}p_{m\mu} = 0 \tag{57d}$$

$$\mathrm{i}\Omega^{(W)}_{m\mu}\big(p_{m\mu} - C^2\rho_{m\mu}\big) + \Big(\frac{DW^2}{r} - C^2 D'\Big)v_{m\mu} = 0 \tag{57e}$$

6.2 Without swirl and variable entropy

$$\mathrm{i}\Omega_{m\mu}\rho_{m\mu} + D\Big(-\mathrm{i}\kappa_{m\mu}u_{m\mu} + \frac{1}{r}\frac{\partial}{\partial r}(r v_{m\mu}) - \frac{\mathrm{i}m}{r}w_{m\mu}\Big) + D' v_{m\mu} = 0 \tag{58a}$$

$$\mathrm{i}D\Omega_{m\mu}u_{m\mu} + DU' v_{m\mu} - \mathrm{i}\kappa_{m\mu}p_{m\mu} = 0 \tag{58b}$$

$$\mathrm{i}D\Omega_{m\mu}v_{m\mu} + \frac{\partial p_{m\mu}}{\partial r} = 0 \tag{58c}$$

$$\mathrm{i}D\Omega_{m\mu}w_{m\mu} - \frac{\mathrm{i}m}{r}p_{m\mu} = 0 \tag{58d}$$

$$\mathrm{i}\Omega_{m\mu}\big(p_{m\mu} - C^2\rho_{m\mu}\big) - C^2 D' v_{m\mu} = 0 \tag{58e}$$

which becomes, after eliminating all variables but $p_{m\mu}$, the equation

$$\frac{\Omega_{m\mu}D}{r}\frac{\partial}{\partial r}\Big(\frac{r}{\Omega_{m\mu}D}\frac{\partial}{\partial r}p_{m\mu}\Big) + \frac{\kappa_{m\mu}U'}{\Omega_{m\mu}}\frac{\partial}{\partial r}p_{m\mu} + \Big(\frac{\Omega^2_{m\mu}}{C^2} - \kappa^2_{m\mu} - \frac{m^2}{r^2}\Big)p_{m\mu} = 0. \tag{58f}$$

6.3 Homentropic without swirl

$$\mathrm{i}\Omega_{m\mu}\rho_{m\mu} + D\Big(-\mathrm{i}\kappa_{m\mu}u_{m\mu} + \frac{1}{r}\frac{\partial}{\partial r}(r v_{m\mu}) - \frac{\mathrm{i}m}{r}w_{m\mu}\Big) = 0 \tag{59a}$$

$$\mathrm{i}D\Omega_{m\mu}u_{m\mu} + DU' v_{m\mu} - \mathrm{i}\kappa_{m\mu}p_{m\mu} = 0 \tag{59b}$$

$$\mathrm{i}D\Omega_{m\mu}v_{m\mu} + \frac{\partial p_{m\mu}}{\partial r} = 0 \tag{59c}$$

$$\mathrm{i}D\Omega_{m\mu}w_{m\mu} - \frac{\mathrm{i}m}{r}p_{m\mu} = 0 \tag{59d}$$

$$p_{m\mu} - C^2\rho_{m\mu} = 0. \tag{59e}$$

This becomes for $p_{m\mu}$ (because D is a constant)

$$\frac{\Omega_{m\mu}}{r}\frac{\partial}{\partial r}\Big(\frac{r}{\Omega_{m\mu}}\frac{\partial}{\partial r}p_{m\mu}\Big) + \frac{\kappa_{m\mu}U'}{\Omega_{m\mu}}\frac{\partial}{\partial r}p_{m\mu} + \Big(\frac{\Omega^2_{m\mu}}{C^2} - \kappa^2_{m\mu} - \frac{m^2}{r^2}\Big)p_{m\mu} = 0. \tag{59f}$$

6.4 Irrotational homentropic flow

$$\mathrm{i}\Omega^{(\Gamma)}_{m\mu}\rho_{m\mu} + D\Big(-\kappa^2_{m\mu}\phi_{m\mu} + \frac{1}{r}\frac{\partial}{\partial r}\big(r\frac{\partial\phi_{m\mu}}{\partial r}\big) - \frac{m^2}{r^2}\phi_{m\mu}\Big) + D'\frac{\partial\phi_{m\mu}}{\partial r} = 0 \tag{60a}$$

$$\mathrm{i}D\Omega^{(\Gamma)}_{m\mu}\phi_{m\mu} + p_{m\mu} = 0 \tag{60b}$$

$$p_{m\mu} - C^2\rho_{m\mu} = 0 \tag{60c}$$

This becomes for $\phi_{m\mu}$

$$\frac{1}{rD}\frac{\partial}{\partial r}\big(rD\frac{\partial\phi_{m\mu}}{\partial r}\big) + \Big(\Big\{\frac{\Omega^{(\Gamma)}_{m\mu}}{C}\Big\}^2 - \kappa^2_{m\mu} - \frac{m^2}{r^2}\Big)\phi_{m\mu} = 0 \tag{60d}$$

6.5 Uniform mean flow with irrotational isentropic perturbations

$$\mathrm{i}\Omega_{m\mu}\rho_{m\mu} + D\Big(-\kappa^2_{m\mu}\phi_{m\mu} + \frac{1}{r}\frac{\partial}{\partial r}\big(r\frac{\partial\phi_{m\mu}}{\partial r}\big) - \frac{m^2}{r^2}\phi_{m\mu}\Big) = 0 \tag{61a}$$

$$\mathrm{i}D\Omega_{m\mu}\phi_{m\mu} + p_{m\mu} = 0 \tag{61b}$$

$$p_{m\mu} - C^2\rho_{m\mu} = 0 \tag{61c}$$

This becomes, finally, for $\phi_{m\mu}$

$$\frac{1}{r}\frac{\partial}{\partial r}\big(r\frac{\partial\phi_{m\mu}}{\partial r}\big) + \Big(\frac{\Omega^2_{m\mu}}{C^2} - \kappa^2_{m\mu} - \frac{m^2}{r^2}\Big)\phi_{m\mu} = 0 \tag{61d}$$

6.6 The modes

The resulting differential equations and boundary conditions are to be solved as eigenvalue problems, with in general complex eigenvalues $\kappa_{m\mu}$. This can be done in various ways that we will not further discuss here. For example, the uniform flow case allows an analytical solution and therefore is a particularly interesting case, but for the other more general cases numerical solution methods are necessary.

In the present application it is very important to distinguish the incoming and outgoing (left- and right-running) waves. The set of poles corresponding to modes decaying in the positive x-direction are found (in this notation convention!) in the lower complex half plane $\mathrm{Im}(\kappa) < 0$. Apart from any instabilities*, these modes are entirely right running. Further, the set of poles corresponding to modes decaying in the negative x-direction are found in the upper complex half plane $\mathrm{Im}(\kappa) > 0$ and apart from any instabilities, these modes are entirely left running. The poles found along the real κ-axis are not immediately recognized as either right or left running. Without mean flow, the direction of the wave corresponds with the modal phase velocity κ_μ/ω. With flow this is not exactly the case anymore and some extra care must be taken. One possible way to classifiy the modes is by taking the hard wall limit of a duct with soft (dissipative) walls.

*Note that a necessary and sufficient condition for stability of a rotating incompressible inviscid fluid is $\frac{\mathrm{d}}{\mathrm{d}r}(Wr)^2 > 0$, (Rayleigh, see [3]).

7 Mode matching

If we have found the modal basis functions of all field variables, both incoming and outgoing, we can write our field as a formal series expansion over these basis functions. Suppose that the *outgoing* basis functions of the pressure $p_{m\mu}$ are the set $\psi_{m\mu}(r)$ with $\mu > 0$ and the *incoming* are the set $\psi_{m\mu}(r)$ with $\mu < 0$.

In the following, we will consider two approaches (see section 4.2). A simpler one (options i or ii) based on direct modal expansion of the interface quantities, where only outgoing modes are considered and a more advanced one (option iii) based on a least squares approach, where outgoing but also incoming modes (option iv) may be included.

The reason for optionally including incoming (*i.e.* reflected) modes, is the imperfect reflection-free boundary condition in the CFD calculations. One way to obtain a reflection-free interface is by modal wave splitting, a procedure similar to the one described here. By including this final step in the matching procedure, the CFD results may be slightly improved. Furthermore, the complexity of the method we propose is just the same if we include incoming modes or not. At present, it is not possible to decide if this option is really useful and a final conclusion should be based on further study.

Under the assumption of completeness, as discussed before, we can write the resulting outgoing pressure field (or any other variable) as

$$p_m(x,r) = \sum_{\mu=1}^{M} A_{m\mu}\psi_{m\mu}(r)\,\mathrm{e}^{-\mathrm{i}\kappa_{m\mu}x} \tag{62}$$

where M is the number of modes considered.

If the pressure is to be continuous at the interface and we do not include possible reflections (that is only in option iv), we have thus

$$\sum_{\mu=1}^{M} A_{m\mu}\psi_{m\mu}(r)\,\mathrm{e}^{-\mathrm{i}\kappa_{m\mu}(x_0+\lambda r)} = \mathcal{P}_m(r) \tag{63}$$

The amplitudes are found by the following Galerkin-type procedure.

Form an (L_2) inner product, between the left and right hand sides and a suitable set of test functions, by integration along the cross section of the interface, *i.e.* between R_1 to R_2. Usually, the complex conjugate of the basis functions themselves are convenient for this purpose, especially when they are orthogonal or nearly orthogonal under the defined inner product. We choose here $\psi^*_{m\nu}(r)\,\mathrm{e}^{\mathrm{i}\kappa^*_{m\nu}\lambda r}$, $\nu = 1\ldots M$, to get

$$\sum_{\mu=1}^{M} A_{m\mu}\,\mathrm{e}^{-\mathrm{i}\kappa_{m\mu}x_0}\int_{R_1}^{R_2}\psi_{m\mu}(r)\psi^*_{m\nu}(r)\,\mathrm{e}^{-\mathrm{i}(\kappa_{m\mu}-\kappa^*_{m\nu})\lambda r}\,r\,\mathrm{d}r = \int_{R_1}^{R_2}\mathcal{P}_m(r)\psi^*_{m\nu}(r)\,\mathrm{e}^{\mathrm{i}\kappa^*_{m\nu}\lambda r}\,r\,\mathrm{d}r \tag{64}$$

or in matrix form

$$\mathcal{M}\boldsymbol{a} = \boldsymbol{p} \tag{65}$$

where

$$\{\mathcal{M}\}_{\nu\mu} = \int_{R_1}^{R_2}\psi_{m\mu}(r)\psi^*_{m\nu}(r)\,\mathrm{e}^{-\mathrm{i}(\kappa_{m\mu}-\kappa^*_{m\nu})\lambda r}\,r\,\mathrm{d}r \tag{66a}$$

$$\{\boldsymbol{a}\}_{\mu} = A_{m\mu}\,\mathrm{e}^{-\mathrm{i}\kappa_{m\mu}x_0} \tag{66b}$$

$$\{\boldsymbol{p}\}_{\nu} = \int_{R_1}^{R_2}\mathcal{P}_m(r)\psi^*_{m\nu}(r)\,\mathrm{e}^{\mathrm{i}\kappa^*_{m\nu}\lambda r}\,r\,\mathrm{d}r \tag{66c}$$

With this choice of test functions the matrix $\mathcal{M}$ is then hermitian. This means that the transposed complex conjugate, *i.e.* $\mathcal{M}^* = \overline{\mathcal{M}}^\top$, is equal to $\mathcal{M}$ itself: $\mathcal{M}^* = \mathcal{M}$, leading to the important consequences that $\mathcal{M}$'s eigenvalues are real and $\mathcal{M}$'s eigenvectors are orthogonal. An even more important consequence here is the relatively simple form that the solution of the least square problem, defined below, attains. Therefore, we will assume in the analysis below that the test functions are chosen such that $\mathcal{M}$ is hermitian.

Now we can construct solutions according to the 4 approaches, proposed in section 4.2.

7.1 Single variable (option i)

Here is the direct way, where only one variable (for example p) is continuous and the other field variables are ignored. As discussed in section 4.2(i), we do not account for false reflections, so we have

$$p_m(x,r) = \sum_{\mu=1}^{M} A_{m\mu}\,\psi_{m\mu}(r)\,\mathrm{e}^{-\mathrm{i}\kappa_{m\mu}x} \tag{67}$$

$$\sum_{\mu=1}^{M} A_{m\mu}\,\mathrm{e}^{-\mathrm{i}\kappa_{m\mu}x_0}\int_{R_1}^{R_2}\psi_{m\mu}(r)\psi^*_{m\nu}(r)\,\mathrm{e}^{-\mathrm{i}(\kappa_{m\mu}-\kappa^*_{m\nu})\lambda r}\,r\,\mathrm{d}r = \int_{R_1}^{R_2}\mathcal{P}_m(r)\psi^*_{m\nu}(r)\,\mathrm{e}^{\mathrm{i}\kappa^*_{m\nu}\lambda r}\,r\,\mathrm{d}r \tag{68}$$

Using the same nomenclature as given by equations (66), the amplitude vector is then (formally) given by

$$\boldsymbol{a} = \mathcal{M}^{-1}\boldsymbol{p} \tag{69}$$

and may be obtained by standard numerical techniques.

7.2 Averaging over several variables (option ii)

Here is the solution averaged over a number of found amplitudes. Assume that we consider pressure, axial velocity or axial pressure gradient, and entropy, with basis functions $\psi_{m\mu}(r)$, $\chi_{m\mu}(r)$, $\zeta_{m\mu}(r)$ respectively. Then we write

$$u_m(x,r) = \sum_{\mu=1}^{M} A^{(u)}_{m\mu}\,\chi_{m\mu}(r)\,\mathrm{e}^{-\mathrm{i}\kappa_{m\mu}x} \tag{70}$$

$$s_m(x,r) = \sum_{\mu=1}^{M} A^{(s)}_{m\mu}\,\zeta_{m\mu}(r)\,\mathrm{e}^{-\mathrm{i}\kappa_{m\mu}x} \tag{71}$$

and determine provisional values of the amplitudes by inner products as before. Hence, we have

$$\sum_{\mu=1}^{M} A^{(p)}_{m\mu}\,\psi_{m\mu}(r)\,\mathrm{e}^{-\mathrm{i}\kappa_{m\mu}(x_0+\lambda r)} = \mathcal{P}_m(r) \tag{72}$$

$$\sum_{\mu=1}^{M} A^{(u)}_{m\mu}\,\chi_{m\mu}(r)\,\mathrm{e}^{-\mathrm{i}\kappa_{m\mu}(x_0+\lambda r)} = \mathcal{U}_m(r) \tag{73}$$

$$\sum_{\mu=1}^{M} A^{(s)}_{m\mu}\,\zeta_{m\mu}(r)\,\mathrm{e}^{-\mathrm{i}\kappa_{m\mu}(x_0+\lambda r)} = \mathcal{S}_m(r) \tag{74}$$

Now we multiply and integrate (although the idea is exactly the same as for equations (66), we will write for clarity now and reference later, all formulas out explicitly) to obtain

$$\sum_{\mu=1}^{M} A_{m\mu}^{(p)}\,\mathrm{e}^{-\mathrm{i}\kappa_{m\mu}x_0}\int_{R_1}^{R_2}\psi_{m\mu}(r)\psi_{m\nu}^{*}(r)\,\mathrm{e}^{-\mathrm{i}(\kappa_{m\mu}-\kappa_{m\nu}^{*})\lambda r}\,r\,\mathrm{d}r=\int_{R_1}^{R_2}\mathcal{P}_m(r)\psi_{m\nu}^{*}(r)\,\mathrm{e}^{\mathrm{i}\kappa_{m\nu}^{*}\lambda r}\,r\,\mathrm{d}r \tag{75}$$

$$\sum_{\mu=1}^{M} A_{m\mu}^{(u)}\,\mathrm{e}^{-\mathrm{i}\kappa_{m\mu}x_0}\int_{R_1}^{R_2}\chi_{m\mu}(r)\chi_{m\nu}^{*}(r)\,\mathrm{e}^{-\mathrm{i}(\kappa_{m\mu}-\kappa_{m\nu}^{*})\lambda r}\,r\,\mathrm{d}r=\int_{R_1}^{R_2}\mathcal{U}_m(r)\chi_{m\nu}^{*}(r)\,\mathrm{e}^{\mathrm{i}\kappa_{m\nu}^{*}\lambda r}\,r\,\mathrm{d}r \tag{76}$$

$$\sum_{\mu=1}^{M} A_{m\mu}^{(s)}\,\mathrm{e}^{-\mathrm{i}\kappa_{m\mu}x_0}\int_{R_1}^{R_2}\zeta_{m\mu}(r)\zeta_{m\nu}^{*}(r)\,\mathrm{e}^{-\mathrm{i}(\kappa_{m\mu}-\kappa_{m\nu}^{*})\lambda r}\,r\,\mathrm{d}r=\int_{R_1}^{R_2}\mathcal{S}_m(r)\zeta_{m\nu}^{*}(r)\,\mathrm{e}^{\mathrm{i}\kappa_{m\nu}^{*}\lambda r}\,r\,\mathrm{d}r \tag{77}$$

or in matrix form

$$\mathcal{M}\boldsymbol{a}^{(p)}=\boldsymbol{p},\quad \mathcal{N}\boldsymbol{a}^{(u)}=\boldsymbol{u},\quad \mathcal{Q}\boldsymbol{a}^{(s)}=\boldsymbol{s} \tag{78}$$

where

$$\{\mathcal{M}\}_{\nu\mu}=\int_{R_1}^{R_2}\psi_{m\mu}(r)\psi_{m\nu}^{*}(r)\,\mathrm{e}^{-\mathrm{i}(\kappa_{m\mu}-\kappa_{m\nu}^{*})\lambda r}\,r\,\mathrm{d}r,\quad \{\boldsymbol{a}^{(p)}\}_{\mu}=A_{m\mu}^{(p)}\,\mathrm{e}^{-\mathrm{i}\kappa_{m\mu}x_0},\quad \{\boldsymbol{p}\}_{\nu}=\int_{R_1}^{R_2}\mathcal{P}_m(r)\psi_{m\nu}^{*}(r)\,\mathrm{e}^{-\mathrm{i}(\kappa_{m\mu}-\kappa_{m\nu}^{*})\lambda r}\,r\,\mathrm{d}r \tag{79}$$

$$\{\mathcal{N}\}_{\nu\mu}=\int_{R_1}^{R_2}\chi_{m\mu}(r)\chi_{m\nu}^{*}(r)\,\mathrm{e}^{-\mathrm{i}(\kappa_{m\mu}-\kappa_{m\nu}^{*})\lambda r}\,r\,\mathrm{d}r,\quad \{\boldsymbol{a}^{(u)}\}_{\mu}=A_{m\mu}^{(u)}\,\mathrm{e}^{-\mathrm{i}\kappa_{m\mu}x_0},\quad \{\boldsymbol{u}\}_{\nu}=\int_{R_1}^{R_2}\mathcal{U}_m(r)\chi_{m\nu}^{*}(r)\,\mathrm{e}^{-\mathrm{i}(\kappa_{m\mu}-\kappa_{m\nu}^{*})\lambda r}\,r\,\mathrm{d}r \tag{80}$$

$$\{\mathcal{Q}\}_{\nu\mu}=\int_{R_1}^{R_2}\zeta_{m\mu}(r)\zeta_{m\nu}^{*}(r)\,\mathrm{e}^{-\mathrm{i}(\kappa_{m\mu}-\kappa_{m\nu}^{*})\lambda r}\,r\,\mathrm{d}r,\quad \{\boldsymbol{a}^{(s)}\}_{\mu}=A_{m\mu}^{(s)}\,\mathrm{e}^{-\mathrm{i}\kappa_{m\mu}x_0},\quad \{\boldsymbol{s}\}_{\nu}=\int_{R_1}^{R_2}\mathcal{S}_m(r)\zeta_{m\nu}^{*}(r)\,\mathrm{e}^{-\mathrm{i}(\kappa_{m\mu}-\kappa_{m\nu}^{*})\lambda r}\,r\,\mathrm{d}r \tag{81}$$

The amplitudes are subsequently

$$\boldsymbol{a}^{(p)}=\mathcal{M}^{-1}\boldsymbol{p},\quad \boldsymbol{a}^{(u)}=\mathcal{N}^{-1}\boldsymbol{u},\quad \boldsymbol{a}^{(s)}=\mathcal{Q}^{-1}\boldsymbol{s} \tag{82}$$

which should be about the same if the discontinuity is not too strong (a point of study!). Finally, we take for the "real" amplitude the average between the three variables

$$\boldsymbol{a}=\tfrac{1}{3}\big(\boldsymbol{a}^{(p)}+\boldsymbol{a}^{(u)}+\boldsymbol{a}^{(s)}\big) \tag{83}$$

7.3 Least squares approach (option iii)

The least squares approach largely follows the steps of option (ii). Instead of equation (78), we now aim at determining $\boldsymbol{a}$ such that it minimizes the cost function

$$c_1\big\|\mathcal{M}\boldsymbol{a}-\boldsymbol{p}\big\|^2+c_2\big\|\mathcal{N}\boldsymbol{a}-\boldsymbol{u}\big\|^2+c_3\big\|\mathcal{Q}\boldsymbol{a}-\boldsymbol{s}\big\|^2. \tag{84}$$

Note that we write $\boldsymbol{u}$ for axial velocity, but this may as well be any other quantity, like axial pressure gradient.

The scaling constants

$$c_1 = \frac{1}{p_{\text{ref}}^2}, \quad c_2 = \frac{1}{u_{\text{ref}}^2}, \quad c_3 = \frac{1}{s_{\text{ref}}^2} \tag{85}$$

are necessary, because the variables are as yet not scaled and therefore not comparable to one another. The actual values of these scalings will need some discussion. A possible choice is $p_{\text{ref}} = \rho_\infty c_\infty^2$, $u_{\text{ref}} = c_\infty$ and $s_{\text{ref}} = [S]_{\text{duct}}$, where $[S]_{\text{duct}}$ is a representative mean entropy variation across the duct. However, if we take for example the axial pressure gradient as a matching variable, we take another scaling accordingly.

If we search for the vector $\boldsymbol{a}$ that minimizes the above cost function (84) and use the hermitian property of $\mathcal{M}$, we get* the following system

$$\left(c_1\mathcal{M}^2 + c_2\mathcal{N}^2 + c_3\mathcal{Q}^2\right)\boldsymbol{a} = c_1\mathcal{M}\,\boldsymbol{p} + c_2\mathcal{N}\,\boldsymbol{u} + c_3\mathcal{Q}\boldsymbol{s} \tag{86}$$

and this equation is easily solved by standard numerical techniques.

7.4 Least squares with reflections (option iv)

If we indicate incoming modes by a negative index μ and include a reflected field at the CFD-side of the interface to the produced field (44), we now have the continuity condition

$$\sum_{\mu=1}^{M} A_{m\mu}\,\psi_{m\mu}(r)\,\mathrm{e}^{-\mathrm{i}\kappa_{m\mu}(x_0+\lambda r)} = \mathcal{P}_m(r) + \sum_{\mu=-1}^{-M} B_{m\mu}\,\psi_{m\mu}(r)\,\mathrm{e}^{-\mathrm{i}\kappa_{m\mu}(x_0+\lambda r)} \tag{87}$$

where $A_{m\mu}$ are the amplitudes of the transmitted modes and $B_{m\mu}$ the amplitudes of the reflected modes. As discussed before, the reflected modes are not relevant to the acoustic regime, but may be useful for polishing up the CFD solution.

Although equation (87) refers physically to a balance between quantities, only valid at their own side of the interface, we can formally rewrite it such that it takes exactly the same form as the equations used in options (i), (ii) and (iii), without reflection. If we identify the amplitudes

$$A_{m\mu} = -B_{m\mu} \quad \text{if} \quad \mu = -1 \ldots - M \tag{88}$$

and bring the reflected field to the left hand side, we obtain

$$\sum_{\mu=-M}^{M} A_{m\mu}\,\psi_{m\mu}(r)\,\mathrm{e}^{-\mathrm{i}\kappa_{m\mu}(x_0+\lambda r)} = \mathcal{P}_m(r) \tag{89}$$

*Introduce the complex vectorial inner product $[\boldsymbol{x}, \boldsymbol{y}]$, which is equal to the ordinary inner product with $\boldsymbol{y}$ complex conjugated: $[\boldsymbol{x}, \boldsymbol{y}] = (\boldsymbol{x}, \overline{\boldsymbol{y}})$. Then the hermitian property of $\mathcal{M}$ implies

$$[\mathcal{M}\boldsymbol{x}, \boldsymbol{y}] = [\boldsymbol{x}, \mathcal{M}^*\boldsymbol{y}] = [\boldsymbol{x}, \mathcal{M}\boldsymbol{y}].$$

Each squared distance in the cost function (84) becomes now like

$$\left\|\mathcal{M}\boldsymbol{a} - \boldsymbol{p}\right\|^2 = [\mathcal{M}\boldsymbol{a} - \boldsymbol{p}, \mathcal{M}\boldsymbol{a} - \boldsymbol{p}] = [\mathcal{M}^2\boldsymbol{a}, \boldsymbol{a}] - [\boldsymbol{a}, \mathcal{M}\boldsymbol{p}] - [\mathcal{M}\boldsymbol{p}, \boldsymbol{a}] + [\boldsymbol{p}, \boldsymbol{p}].$$

If we vary around $\boldsymbol{a}$ by substituting $\boldsymbol{a} + \varepsilon\boldsymbol{b}$, we find for $O(\varepsilon)$ that the variation of $\left\|\mathcal{M}\boldsymbol{a} - \boldsymbol{p}\right\|^2$ is

$$2\,\mathrm{Re}\{[\mathcal{M}^2\boldsymbol{a} - \mathcal{M}\boldsymbol{p}, \boldsymbol{b}]\}.$$

If we look for stationary values of cost function (84) for any vector $\boldsymbol{b}$, the result (86) for $\boldsymbol{a}$ is obtained.

with $\mu = 0$ excluded. (Similar for other variables.) From here on the problem can be solved in the same way as under option (iii), with the only difference that the size of the vectors and matrices are $2M$ and $2M \times 2M$ respectively.

How does this compare with traditional mode matching?

It is interesting to compare this least squares approach with the traditional mode matching. In traditional mode matching only two variables, pressure p and axial velocity u, are made continuous. However, with $2M$ unknowns (the transmitted and reflected amplitudes), only $2M$ equations are necessary. These are created by taking L_2 inner products of the continuity equations for p and u, like equation (64), but not with all $2M$ basis functions. Only M basis functions from the p expansion (for example, the outgoing modes) are applied to the continuity of pressure, leading to M equations. Similarly, M basis function from the u expansion are applied to the continuity of velocity. Together, we have $2M$ equations, yielding uniquely the $2M$ unknown amplitudes.

In our least squares approach of option (iv) we create even more equations, so that in the case of 2 variables we have $4M$ equations. With only $2M$ unknowns, these equations cannot in general be satisfied exactly and therefore we use the least squares method. So the least squares solution is an *approximation*.

It should be noted, however, that unless the basis functions are L_2-orthogonal, the amplitudes found by the traditional method are also an approximation. They depend on the number of modes M and on the chosen basis functions used for the inner products. Only when $M \to \infty$ do the amplitudes converge to the (a?) "correct" value.

So in general the least squares solution will differ from the traditional mode matching solution. However, as the standard solution produces a small jump across the interface, the least squares solution (constructed to minimize this jump) will naturally differ only by a small amount.

Further, there is *no* difference when the problem is symmetric and the left and right running modes are equivalent. In that case only $2M$ equations are different and the least squares solution will be equivalent to the traditional mode matching solution (the least squares residue is exactly zero). In the general, a-symmetric case, the least squares solution is expected to be slightly better. The inner product equations are better balanced, because there is no dependence on the choice of the basis functions (all are used).

Since the least squares solution is not restricted to only 2 variables, incorporates very easily any number of continuity conditions and the formulas, utilizing the hermitian form of the matrices, are very simple, the least squares approach seems to be superior to the traditional approach.

7.5 Other basis functions

We used modal basis functions for the matching, because these modes are each solutions of the differential equations (in the assumed constant duct section) and therefore allows us to distinguish between incoming and outgoing waves. If this information is not important or usable, for example because the acoustic model only needs (ω, m)-profiles of the pressure perturbations at the interface, it is possible to use other types of basis functions, as long as no manipulations are included that use the direction of the field (*e.g.* no wave splitting).

7.6 Conclusion

Once the matrices $\mathcal{M}, \mathcal{N}, \mathcal{Q}$ are determined, the least squares method is only little more complicated than the average method. Therefore, we consider it to be the preferred method.

Note that it is not clear yet in all possible situations which acoustic variables are the relevant ones to be included.

The question whether option (iv) is to be preferred over option (iii) depends on the quality of the CFD field and this should be tested in practice.

8 General strategy

Summarizing the proposed strategy step by step, we have

1. Consider the geometry. The interface should be located in a part of the duct that can be approximated (locally) by a cylindrical straight duct. The mean flow should be (approximately) axisymmetric.

   Sensitivity of the matching to the position of the interface should be included in the tests.

2. The total flow field, produced by the CFD calculations at the interface, has to be split into the steady part (the mean flow) and the unsteady part for each multiple $\omega = n\Omega$ of the first harmonic Ω and circumferential m-mode considered (the perturbations). A logical approach is via Fourier transformations in t and θ, after which all frequencies and m-modes of interest are available. If the mean flow is not axisymmetric (*i.e.* θ-dependent), the $m = 0$-component is automatically its average over θ.

   So from a physical quantity $f(x, r, \theta, t)$, given at the interface $x_i(r) = x_0 + \lambda r$, we derive the mean flow quantity $F(r)$ and the (m, ω)-Fourier component $\mathcal{F}_m(r; \omega)$ of the acoustic interface quantity as follows. If f is periodic in time with period $2\pi/\Omega$ (radial frequency Ω), it can be written as

$$f(x_i, r, \theta, t) = \sum_{n=-\infty}^{\infty} \sum_{m=-\infty}^{\infty} \hat{f}_m(r; n\Omega)\, \mathrm{e}^{\mathrm{i}n\Omega t - \mathrm{i}m\theta} \tag{90}$$

   Each Fourier component is given by

$$\hat{f}_m(r; n\Omega) = \frac{\Omega}{4\pi^2} \int_0^{2\pi} \int_0^{2\pi/\Omega} f(x_i, r, \theta, t)\, \mathrm{e}^{\mathrm{i}m\theta - \mathrm{i}n\Omega t}\, \mathrm{d}t\, \mathrm{d}\theta \tag{91}$$

   (Note the $\pm\mathrm{i}$ and 2π conventions!). We have then (*c.f.* equation 23, 46)

$$F(r) = \hat{f}_0(r; 0) \tag{92a}$$

$$\mathcal{F}_m(r; \omega) = \hat{f}_m(r; \omega) \tag{92b}$$

   If the CFD results refer to a single rotor stage, they are effectively steady in a co-rotating frame of reference. If, in addition, the field is periodic in θ with period $2\pi/B$ (B blades, say), the above Fourier transformation may be simplified as follows. We write our field function as

$$f(x_i, r, \theta, t) = g(x_i, r, \theta - \Omega t) = \sum_{n=-\infty}^{\infty} \sum_{m=-\infty}^{\infty} \hat{g}_m(r; n\Omega)\, \mathrm{e}^{\mathrm{i}n\Omega t - \mathrm{i}mB\theta} \tag{93}$$

Now the double Fourier integrals reduce to a single one, while most of the Fourier coefficients $\hat{g}_m(r; n\Omega)$ vanish:

$$\hat{g}_m(r; n\Omega) = \frac{1}{2\pi}\delta_{n,mB}\int_0^{2\pi} g\left(x_i, r, \tfrac{\xi}{B}\right) \mathrm{e}^{\mathrm{i}\xi}\ \mathrm{d}\xi\ . \tag{94}$$

3. The mean flow variables will not form a consistent solution of the mean flow equations that corresponds to the acoustic model considered. Depending on the model, the mean flow is to be "stripped" by means of averaging until the mean flow variables are consistent. This means that a swirl may be simplified or ignored, or that the radial pressure distribution is to be adjusted to a given swirl and density distribution. As this mean-flow post-processing depends on the acoustic model considered, we will not prescribe here a preferred procedure. Therefore, one should be careful always to attach to any results the definitions used, which should be described explicitly and in sufficient detail.

4. Once the mean flow is known, the acoustic modal equations can be solved for the circumferential mode numbers m of interest and the matrices $\mathcal{M}$, *etc.*., can be formed using the available basis functions.

5. The perturbation field has to be decomposed into circumferential Fourier modes, leading to field quantities that only depend on r.

6. The vectors $\boldsymbol{p}$, etc., can be constructed from the field and the basis functions.

7. A selection should be made which acoustic variables are considered to be most relevant and should be made as continuous as possible. Pressure p and axial velocity u seem to be suitable for the inlet. Care is necessary in case of dominating vorticity downstream of a rotor or stator. In that case it might be better to take the pressure and the axial component of the pressure gradient. If the mean flow contains swirl, while the acoustic model includes that feature, the radial or circumferential velocities v or w or, alternatively, the rotation $\boldsymbol{\xi} = \nabla\times\boldsymbol{v}$, might be included. If radial temperature variations could produce entropy modes, the entropy should be included.

   Note that this item is not clear yet and ought to be subject to further research.

8. The least squares calculations can be performed to obtain the amplitude vectors. A measure of the model-jump, *i.e.* the discrepancy between the neighbouring CFD and CAA models, may be represented by the residual least-squares error, or the amount of spurious reflections.

Part B:

A Preliminary Report on Matching Strategy and Radiation Model

Xin Zhang
University of Southampton,
Southampton SO17 1BJ, U.K.
March 8, 2001

Abstract

In this preliminary report, an approach taken by ISVR on the TurboNoiseCFD project bypass/exhaust duct noise radiation calculation is described. The ISVR model consists of a wave admission region, a computational aeroacoustic (CAA) region and a radiation model based on an integral solution of the Ffowcs Williams-Hawkings (FW-H) equation implemented numerically to allow near- and far-field noise levels to be determined efficiently. The wave admission region is designed to allow for the matching of incoming acoustic waves with the CAA region. At this stage of the project research, a number of issues need to be addressed so that the model can be validated and used in the TurboNoiseCFD project.

Nomenclature

c_0	Freestream speed of sound
E	Total energy
$f(\mathbf{x}, t) = 0$	Equation of integration surface
$H(f)$	Heaviside function
M	Mach number
M_r	Mach number in the radiation direction
$\hat{\mathbf{n}}$	Unit outward normal vector to surface $f = 0$
p	Pressure
p'	Perturbation pressure
P_0	Mean pressure
r	Length of radiation vector, $\|\mathbf{x} - \mathbf{y}\|$
$\mathbf{r}$	Radiation vector, $\mathbf{x} - \mathbf{y}$

$\hat{\mathbf{r}}$	Unit radiation vector, $\mathbf{r}/r$
t	Observer time
u	x-direction velocity
u'	Perturbation x-direction velocity
$\mathbf{u}$	Flow velocity vector
U_0	Mean x-direction velocity
v	y-direction velocity
v'	Perturbation y-direction velocity
v_r	Projection of flow velocity in radiation direction
$\mathbf{v}$	Integration surface velocity vector
V_0	Mean y-direction velocity
w	z-direction velocity
w'	Perturbation z-direction velocity
W_0	Mean z-direction velocity
x, y, z	Cartesian coordinates
$\mathbf{x}$	Far-field observer position vector
$\mathbf{y}$	Source position vector

Greek Symbols

$\delta(f)$	Dirac delta function
δ_{ij}	Kronecker delta function
ρ	Density
ρ'	Perturbation density
ρ_0	Mean density
τ	Source time
ξ, η, ζ	Transformed coordinates

9 Introduction

In the TurboNoiseCFD project, a part of ISVR's effort is to develop a model of noise radiation from the aft bypass and exhaust ducts. It involves admission of noise propagation from the rotor and OGV, though the ducts into the exhaust flow region, and transmission of noise in the exhaust/jet flow region, leading to the far-field noise radiation. Consortium partners using computational fluid dynamics (CFD) generate the unsteady flow/noise data. The data are further analysed and would be available in the forms of various wave inputs, *i.e.* acoustic, vorticity and entropy. The noise generated by the exhaust/jet flow itself is not considered at this stage.

A major issue is the admission of waves into the aerodynamic flow region covered by the ISVR effort, *i.e.* flow outside the bypass and exhaust ducts. A matching problem is most likely to occur across the interface between the duct region and bypass/exhaust flow region, as two different flow solvers are likely to be used. On the interface, dynamically balanced flow solutions produced by one solver (*e.g.* Navier-Stokes) cannot be directly used as the inflow conditions for another flow solver (*e.g.* Linearised Euler), due to different approximations in the governing equations.

10 Proposed Radiation Model

The proposed model consists of three parts as illustrated in figure 3 with a simple schematic: wave admission region, CAA region and radiation region. In the wave admission region, the incoming waves from the TUE duct acoustic calculations are admitted into the CAA region, in the form defined in the following sections. The wave admission region is in fact a part of the CAA modelling. However, the acoustic waves are prescribed. This region overlaps with a part of the TUE duct acoustic region. Spurious waves and unwanted reflections are damped by a buffer zone boundary condition. In the CAA region, a mean flow model is used to model the exhaust flow out of the bypass/exhaust ducts. The acoustic wave propagation is calculated by a Linearised Euler solver. Solutions from the Linearised Euler equations provide input to the radiation model. In this study, we use a an integral solution of the Ffowcs Williams-Hawkings (FW-H) equation.

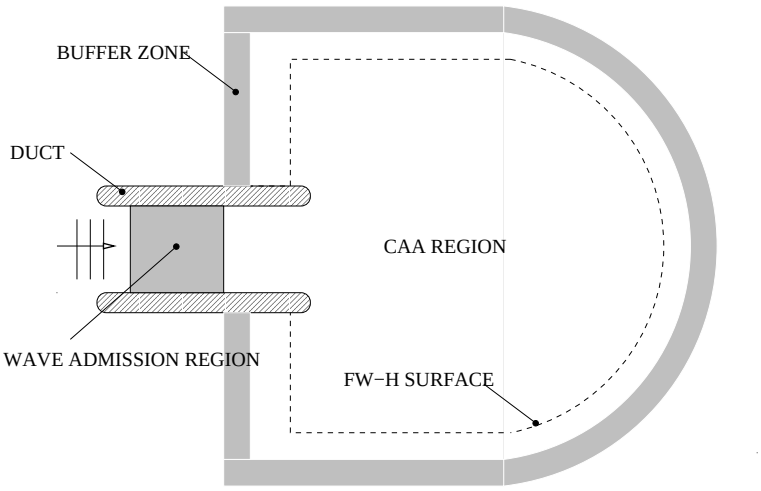

Figure 3: Schematic of the matching and radiation model.

11 Wave Admission Region

There will not be a matching problem for the incoming mean flow in the wave admission region as ISVR will develop a mean flow model for the matching and radiation problem in this project. It is most likely though that there will be a matching problem for the admission of the incoming acoustic waves. The incoming acoustic waves are produced by computational fluid dynamics (CFD) computations and are further processed by duct acoustic calculations (at TUE). The CAA solver used by ISVR possesses low dissipation and dispersion characteristics. Hence any inconsistency at the inflow boundary will introduce errors/spurious wave reflections in the CAA calculations, which will eventually render the calculations useless.

To address the matching problem, a wave admission region is placed inside the duct (see fig.3), which overlaps with the TUE duct acoustic region. Hence the TUE calculations provide not only the wave condition on the inlet of the ISVR wave admission region, but also a ‘target’ for the CAA calculation in the wave admission region. In the wave admission region, the incoming/outgoing waves act as a reference and any corresponding outgoing/incoming waves will be damped. In the incoming flow region, ISVR

requires information of the incoming waves such as angular frequency and axial/circumferential wave number in order to exclude the incoming wave while damping outgoing waves in the region. Therefore, the incoming acoustic waves in the whole of the wave admission region are required. A suitable form would be:

$$f(x,y,z,t) = \sum_{j=-\infty}^{\infty}\sum_{k=-\infty}^{\infty}\sum_{m=-\infty}^{\infty}\sum_{n=-\infty}^{\infty} f_{jkmn} e^{\mathrm{i}n\omega t - \mathrm{i}jk_x x - \mathrm{i}kk_y y - \mathrm{i}mk_z z} \tag{95}$$

where f represents any of density, velocity components and pressure. ω, k_x, k_y, k_z are the angular frequency and x, y, z-direction wave numbers respectively. j, k, n and m are the corresponding wave modes.

The length of this region will be decided through a series of tests. Specifications are be provided in the later stages of the project.

12 CAA Region

12.1 Introduction

In this project, we assume that the acoustic propagation is governed by the Linearised Euler Equations (LEE) where the assumption of small amplitude perturbations about a steady mean flow describes the features of the propagating acoustic waves. In order for a finite difference CAA scheme to capture the same wave propagation characteristics (namely, nondispersive, nondissipative and isotropic) as the solutions of the LEE, the CAA scheme must be of high-order accuracy.

12.2 Summary of equations for fluid motion

Conservation laws

The non-linear Euler Equations representing inviscid and adiabatic fluid motion are represented in a standard strong conservation form in equation (96).

$$\frac{\partial \mathbf{Q}}{\partial t} + \frac{\partial \mathbf{F}}{\partial x} + \frac{\partial \mathbf{G}}{\partial y} + \frac{\partial \mathbf{H}}{\partial z} = 0 \tag{96}$$

where the solution vector $\mathbf{Q}$ is given by

$$\mathbf{Q} = \begin{pmatrix} \rho \\ \rho u \\ \rho v \\ \rho w \\ \rho E \end{pmatrix}$$

and the flux vectors given by

$$\mathbf{F} = \begin{pmatrix} \rho u \\ \rho u^2 + p \\ \rho vu \\ \rho wu \\ u(\rho E + p) \end{pmatrix}, \quad \mathbf{G} = \begin{pmatrix} \rho v \\ \rho uv \\ \rho v^2 + p \\ \rho wv \\ v(\rho E + p) \end{pmatrix}, \quad \mathbf{H} = \begin{pmatrix} \rho w \\ \rho uw \\ \rho vw \\ \rho w^2 + p \\ w(\rho E + p) \end{pmatrix}$$

Formulation of the Linearised Euler Equations (LEE)

For fluid flows where the flow properties can be modeled as unsteady perturbations superimposed on a steady mean flow, ie.

$$\begin{aligned}
\rho(x,y,z,t) &= \rho_0(x,y,z) + \rho'(x,y,z,t),\\
u(x,y,z,t) &= U_0(x,y,z) + u'(x,y,z,t),\\
v(x,y,z,t) &= V_0(x,y,z) + v'(x,y,z,t),\\
w(x,y,z,t) &= W_0(x,y,z) + w'(x,y,z,t),\\
p(x,y,z,t) &= P_0(x,y,z) + p'(x,y,z,t).
\end{aligned} \tag{97}$$

we can linearise for small amplitudes and subsequently obtain the governing equations for the perturbations - the Linearised Euler Equations. Equations (98 - 102) represent the governing perturbation equations about a steady, non-uniform mean flow. The equations have been written in a compact form where a subscript denotes a partial derivative with respect to the subscript variable.

Continuity

$$\begin{aligned}
&\rho'_t + \rho_0\left(u'_x + v'_y + w'_z\right) + U_0\rho'_x + V_0\rho'_y + W_0\rho'_z\\
&\quad = -\rho'\left(U_{0x} + V_{0y} + W_{0z}\right) - \left(u'\rho_{0x} + v'\rho_{0y} + w'\rho_{0z}\right)
\end{aligned} \tag{98}$$

X-momentum

$$\begin{aligned}
&\rho_0 u'_t + \rho_0 U_0 u'_x + \rho_0 V_0 u'_y + \rho_0 W_0 u'_z + p'_x\\
&\quad = -\rho'\left(U_0 U_{0x} + V_0 U_{0y} + W_0 U_{0z}\right) - \rho_0 u' U_{0x} - \rho_0 v' U_{0y} - \rho_0 w' U_{0z}
\end{aligned} \tag{99}$$

Y-momentum

$$\begin{aligned}
&\rho_0 v'_t + \rho_0 U_0 v'_x + \rho_0 V_0 v'_y + \rho_0 W_0 v'_z + p'_y\\
&\quad = -\rho'\left(U_0 V_{0x} + V_0 V_{0y} + W_0 V_{0z}\right) - \rho_0 u' V_{0x} - \rho_0 v' V_{0y} - \rho_0 w' V_{0z}
\end{aligned} \tag{100}$$

Z-momentum

$$\begin{aligned}
&\rho_0 w'_t + \rho_0 U_0 w'_x + \rho_0 V_0 w'_y + \rho_0 W_0 w'_z + p'_z\\
&\quad = -\rho'\left(U_0 W_{0x} + V_0 W_{0y} + W_0 W_{0z}\right) - \rho_0 u' W_{0x} - \rho_0 v' W_{0y} - \rho_0 w' W_{0z}
\end{aligned} \tag{101}$$

Energy

$$\begin{aligned}
&p'_t + U_0 p'_x + V_0 p'_y + W_0 p'_z + \gamma P_0\left(u'_x + v'_y + w'_z\right)\\
&\quad = -u' P_{0x} - v' P_{0y} - w' P_{0z} - \gamma p'\left(U_{0x} + V_{0y} + W_{0z}\right)
\end{aligned} \tag{102}$$

12.3 Implementation of the CAA scheme

Equations (98 - 102) represent the linearised Euler Equations in Cartesian coordinates. The governing equations are recast in generalised curvilinear coordinates that allows the transformation of a curvilinear grid in the physical domain to a rectangular grid in the computational domain. The LEE CAA solver supports the propagation of incoming acoustic, entropy and vorticity waves. Matching the form of the acoustic waves generated in the CFD solvers to the correct form for the LEE is an important task and has been highlighted in this report. Once the correct form of the incoming acoustic waves is determined, the

only other input required for the LEE solver is the mean flow field. In a simple case this can be generated using either an analytic mean flow profile or time-averaged solutions of the Navier-Stokes Equations for the flow within the CAA field.

The LEE solver uses a 6th-order compact scheme for the spatial derivatives and a 4/6 stage explicit Runge-Kutta scheme for the time integration. The solver outputs the temporal and spatial variations of the unsteady flow perturbations (ρ', u', v', w', p'). These act as the input to the Ffowcs-Williams Hawkings solver.

13 Ffowcs Williams-Hawkings Solver

13.1 Introduction

An integral solution of the Ffowcs Williams-Hawkings[13] (FW-H) equation is implemented numerically to allow near- and far-field noise levels to be determined efficiently. The FW-H formulation is particularly attractive in comparison to other integral methods as it permits the passage of hydrodynamic disturbances through the integration surface without effecting the acoustic field, and therefore affords a greater degree of flexibility in positioning the surface than say the Kirchhoff method [9]. The particular integral solution implemented is known as formulation 1A of Farassat[14]. This time-domain formulation is valid in both the near- and far-field, and is appropriate for surfaces in arbitrary motion.

The program described herein is a post-processing piece of software requiring as input the time histories of the flow-field variables ρ, ρu, ρv, ρw and ρE over a user definable integration surface. Normally this is provided in the form of time-accurate CFD data. In such cases the software first interpolates the data to the integration surface before commencing calculations.

13.2 Governing Equations

The FW-H equation may be written in differential form as

$$\Big(\frac{\partial^2}{\partial t^2} - c_o^2\frac{\partial^2}{\partial {x_i}^2}\Big)\big(H(f)\rho'\big) = \frac{\partial^2}{\partial x_i \partial x_j}\big(T_{ij}H(f)\big) - \frac{\partial}{\partial x_i}\big(L_i\delta(f)\big) + \frac{\partial}{\partial t}\big(U\delta(f)\big) \tag{103}$$

where

$$T_{ij} = \rho u_i u_j + P_{ij} - c_o^2\rho'\delta_{ij} \tag{104}$$

$$L_i = \big(P_{ij} + \rho u_i(u_j - v_j)\big)\frac{\partial f}{\partial x_j} \tag{105}$$

$$U = \big(\rho_o v_i + \rho(u_i - v_i)\big)\frac{\partial f}{\partial x_i} \tag{106}$$

The first term T_{ij} is known as the Lighthill stress tensor, and represents the volume sources; the second represents the sound generated by unsteady forces; and the third represents the sound generated as a result of the unsteady mass flux. The FW-H equation is the most general form of the Lighthill acoustic analogy and is appropriate when sound is generated by surfaces in arbitrary motion.

A time-domain solution to the above inhomogeneous second-order partial differential equation is obtained in terms of a Green's function [15]. The Green's function, $G(\mathbf{x}, t; \mathbf{y}, \tau)$ is defined such that it satisfies the wave equation

$$\Big(\frac{\partial^2}{\partial x_i \partial x_i} - \frac{\partial^2}{\partial t^2}\Big) G(\mathbf{x}, t; \mathbf{y}, \tau) = -\delta(t-\tau)\delta(\mathbf{x}-\mathbf{y}) \tag{107}$$

The Green's function $G(\mathbf{x}, t; \mathbf{y}, \tau)$ may be thought of as representing the pressure at point $\mathbf{x}$ and time t caused by an impulsive source located at the point $\mathbf{y}$ and triggered at time τ. The acoustic density fluctuation $\rho'(\mathbf{x}, t)$ perceived by the far-field observer at $\mathbf{x}$ at time t, due to the distribution of sound sources within the volume V and over the surface S, is given by the sum of contributions from all acoustic sources within V and over S at the earlier(retarded) time $\tau = t - \|\mathbf{x}-\mathbf{y}\|/c_\infty$.

A solution of equation 103 can be written as the convolution of the Green's function and the right hand side of the FW-H equation. Using the free-space Green's function, the solution may be written

$$4\pi p'(\mathbf{x}, t) = \frac{\partial^2}{\partial x_i \partial x_j} \int_V \Big[\frac{T_{ij}}{r|1-M_r|}\Big]_{\text{ret}} \mathrm{d}\mathbf{y}^3 + \frac{\partial}{\partial t}\int_s \Big[\frac{\rho'(u_n - v_n) + \rho_o u_n}{r|1-M_r|}\Big]_{\text{ret}} \mathrm{d}\mathbf{S} - \frac{\partial}{\partial x_i}\int_S \Big[\frac{\sigma'_{ij}\hat{n}_j - \rho u_i(u_n - v_n)}{r|1-M_r|}\Big]_{\text{ret}} \mathrm{d}\mathbf{S} \tag{108}$$

Following Farassat the speed and accuracy of the calculation may be improved by converting the spatial derivative of the third integral to a time derivative and then by moving the time derivatives inside the integrals. The first aspect of this is achieved using the relation

$$\frac{\partial}{\partial x_i}\Big(\frac{\delta(g)}{4\pi r}\Big) = \frac{1}{c_0}\frac{\partial}{\partial t}\Big(\frac{\hat{r}_i \delta(g)}{4\pi r}\Big) - \frac{\hat{r}_i \delta(g)}{4\pi r^2} \tag{109}$$

To allow the time derivatives to be taken inside the integral, it is noted that the $r = \|\mathbf{x} - \mathbf{y}(\tau)\|$ is a function of τ and therefore

$$\frac{\partial}{\partial t} = \Big[\frac{1}{1-M_r}\frac{\partial}{\partial \tau}\Big]_{\text{ret}} \tag{110}$$

To complete the derivation, we make use of the following useful relations

$$\frac{\partial r}{\partial \tau} = -v_r \tag{111}$$

$$\frac{\partial \hat{r}_i}{\partial \tau} = \frac{\hat{r}_i v_r - v_i}{r} \tag{112}$$

$$\frac{\partial M_r}{\partial \tau} = \frac{1}{c_0 r}\Big(r_i \frac{\partial v_i}{\partial \tau} + v_r^2 - v^2\Big) \tag{113}$$

$$\frac{\partial U_n}{\partial \tau} = \Big(\frac{\partial U_i}{\partial \tau}\hat{n}_i + U_i \frac{\partial \hat{n}_i}{\partial \tau}\Big) \equiv \dot{U}_n + U_{\dot{n}} \tag{114}$$

The final result is

$$p'(\mathbf{x}, t) = p'_Q(\mathbf{x}, t) + p'_L(\mathbf{x}, t) + p'_T(\mathbf{x}, t) \tag{115}$$

where

$$4\pi p'_T(\mathbf{x}, t) = \int_S \Big[\frac{\rho_0(\dot{U}_n + U_{\dot{n}})}{r(1-M_r)^2}\Big]_{\text{ret}} \mathrm{d}S + \int_S \Big[\frac{\rho_0 U_n(r\ \dot{M}_r + c_0 M_r - c_0 M^2)}{r^2(1-M_r)^3}\Big]_{\text{ret}} \mathrm{d}S \tag{116}$$

$$4\pi p'_L(\mathbf{x},t) = \frac{1}{c_0}\int_S \left[\frac{\dot{L}_r}{r(1-M_r)^2}\right]_{\text{ret}} \mathrm{d}S + \int_S \left[\frac{L_r - L_M}{r^2(1-M_r)^2}\right]_{\text{ret}} \mathrm{d}S + \frac{1}{c_0}\int_S \left[\frac{L_r(r\ \dot{M}_r + c_0 M_r - c_0 M^2)}{r^2(1-M_r)^3}\right]_{\text{ret}} \mathrm{d}S \quad (117)$$

and the term $p'_Q(\mathbf{x},t)$, accounting for the quadrupole sources outside the integration surface, is neglected. This integral representation of the FW-H equation is known as formulation 1A of Farassat.

14 Summary

The matching method and radiation model as proposed in this preliminary report represent some initial thoughts of the bypass and exhaust duct noise matching and propagation problem. A number of issues need to be addressed before the model can be validated and used in the TurboNoiseCFD project.

Bibliography

[1] V.V. GOLUBEV, H.M. ATASSI, Sound propagation in an annular duct with mean potential swirling flow, *Journal of Sound and Vibration*, 1996, **198** (5), p. 601–616

[2] V.V. GOLUBEV, H.M. ATASSI, Acoustic-vorticity waves in swirling flows, *Journal of Sound and Vibration*, 1998, **209** (2), p. 203–222

[3] C.K.W. TAM, L. AURIAULT The wave modes in ducted swirling flows, *Journal of Fluid Mechanics*, 1998, **371**, p. 1–20, (*AIAA-98-2280*)

[4] B. EL-HADIDI, H.M. ATASSI, E. ENVIA, G. PODBOY Evolution of rotor wake in swirling flow, *AIAA-2000-1991*

[5] J.L. KERREBROCK Small disturbances in turbomachinery annuli with swirl, *AIAA Journal*, 1977, **15**(6), p. 794–803

[6] K.A. KOUSEN Eigenmode analysis of ducted flows with radially dependent axial and swirl components, *CEAS/AIAA-95-160*

[7] K.A. KOUSEN Pressure modes in Ducted Flows with Swirl, *AIAA/CEAS-96-1679*

[8] D.P. LOCKARD, An overview of computational aeroacoustic modeling at NASA Langley, *Journal of Computational Physics*, 2000, to appear

[9] B.A. SINGER, K.S. BRENTNER, D.P. LOCKARD, G.M. LILLEY, Simulation of acoustic scattering from a trailing edge, *AIAA-99-0231*, 1999

[10] R.P. DOUGHERTY A parabolic approximation for flow effects on sound propagation in nonuniform softwall ducts, *AIAA-99-1822*, 1999

[11] R.P. DOUGHERTY A wave splitting technique for nacelle acoustic propagation, *AIAA-97-1652*, 1997

[12] L.D. LANDAU AND E.M. LIFSHITZ, Fluid Mechanics, 2nd edition, Pergamon Press, Oxford, 1987

[13] J.E. FFOWCS WILLIAMS AND D.L. HAWKINGS, Sound Generation by Turbulence and Surfaces in Arbitrary Motion, *Philosophical Transactions of The Royal Society, London*, 1969, **246**, p. 321–342

[14] F. FARASSAT AND G.P. SUCCI, The Prediction of Helicopter Discrete Frequency Noise, *Vertica*, 1983, **7**, p. 309–320

[15] M.E. GOLDSTEIN, Aeroacoustics, McGraw-Hill Book Company, Inc., New York, 1976